



A microenvironment-inspired synthetic three-dimensional model for pancreatic ductal adenocarcinoma organoids

Christopher R. Below^{1,2}, Joanna Kelly¹, Alexander Brown³, Jonathan D. Humphries^{2,11}, Colin Hutton¹, Jingshu Xu¹, Brian Y. Lee¹, Celia Cintas¹, Xiaohong Zhang¹, Victor Hernandez-Gordillo³, Linda Stockdale³, Matthew A. Goldsworthy⁴, Joe Geraghty⁴, Lucy Foster⁴, Derek A. O'Reilly⁴, Barbara Schedding⁵, Janet Askari², Jessica Burns², Nigel Hodson⁶, Duncan L. Smith¹, Catherine Lally¹, Garry Ashton¹, David Knight⁷, Aleksandr Mironov⁸, Antonia Banyard¹, Johannes A. Eble⁵, Jennifer P. Morton^{9,10}, Martin J. Humphries¹², Linda G. Griffith³✉ and Claus Jørgensen¹✉

Experimental in vitro models that capture pathophysiological characteristics of human tumours are essential for basic and translational cancer biology. Here, we describe a fully synthetic hydrogel extracellular matrix designed to elicit key phenotypic traits of the pancreatic environment in culture. To enable the growth of normal and cancerous pancreatic organoids from genetically engineered murine models and human patients, essential adhesive cues were empirically defined and replicated in the hydrogel scaffold, revealing a functional role of laminin-integrin α_3/α_6 signalling in establishment and survival of pancreatic organoids. Altered tissue stiffness—a hallmark of pancreatic cancer—was recapitulated in culture by adjusting the hydrogel properties to engage mechano-sensing pathways and alter organoid growth. Pancreatic stromal cells were readily incorporated into the hydrogels and replicated phenotypic traits characteristic of the tumour environment in vivo. This model therefore recapitulates a pathologically remodelled tumour microenvironment for studies of normal and pancreatic cancer cells in vitro.

Tumour cells are embedded in a complex environment encompassing conscripted host cells and a pathologically remodelled extracellular matrix (ECM)^{1,2}. Coerced host cells such as immature myeloid cells and macrophages promote the development of an immune suppressive environment, and cancer-associated fibroblasts (CAFs) deposit and remodel the ECM, resulting in a rigid and poorly perfused microenvironment^{3,4}. These features are particularly prominent in pancreatic ductal adenocarcinoma (PDA), where the stromal reaction constitutes, on average, 80% of the total tumour volume^{2,5}. Normalizing the dysfunctional microenvironment improves therapeutic efficiency, where targeting the stiff ECM or the stromal infiltrate improves efficacy of gemcitabine and immune-checkpoint inhibitors^{6–9}. Models that faithfully replicate the stromal environment are therefore essential to improve the development of therapeutic strategies.

A diverse range of preclinical models, including cell lines, genetically engineered murine models and patient-derived xenografts have been instrumental for target discovery and validation. Recently, organoids have gained traction as a complementary model system, enabling the establishment and three-dimensional (3D) culture of murine and patient-derived tumour cells at

high efficiency^{10–12}. However, organoid models are typically established in animal-derived hydrogels, most prominently the basement membrane (BM) extract Matrigel, which suffers from batch-to-batch variability and ill-defined composition, disfavours stromal cell propagation and mostly fails to replicate the pathological ECM of human cancers^{11,13–15}. Consequently, interdependencies between tumour cells and the microenvironment are inadequately modelled in this system. Contemporary synthetic scaffolds, such as the hydrogel scaffolds based on polyethylene glycol (PEG), offer several advantages to cell- and tissue-derived matrices, including exquisite control over growth conditions^{16–19}. Although current model systems have been successfully used for primary and induced pluripotent stem cell-derived intestinal organoids^{16–19}, matrices with tissue-matched adhesion characteristics capable of supporting both epithelial organoids and stromal cells are needed to better replicate the complexity of the tumour ecosystem.

Here, we set out to develop a rationally designed, synthetic 3D model for pancreatic organoids that simultaneously captures relevant physiological components of the tissue microenvironment. We envisaged that an ideal model would replicate essential cell–ECM interactions, mimic tissue stiffness ranges observed across normal

¹Cancer Research UK Manchester Institute, The University of Manchester, Manchester, UK. ²Wellcome Centre for Cell-Matrix Research, Faculty of Biology, Medicine and Health, The University of Manchester, Manchester, UK. ³Centre for Gynepathology Research, Department of Biological Engineering, Massachusetts Institute of Technology, Cambridge, MA, USA. ⁴Manchester Royal Infirmary, Manchester, UK. ⁵Institute for Physiological Chemistry and Pathobiochemistry, University of Muenster, Muenster, Germany. ⁶BioAFM Laboratory, Bioimaging Core Facility, Faculty of Biology, Medicine and Health, The University of Manchester, Manchester, UK. ⁷Biological Mass Spectrometry Core Facility, Faculty of Biology, Medicine and Health, The University of Manchester, Manchester, UK. ⁸Electron Microscopy Core Facility, Faculty of Biology, Medicine and Health, The University of Manchester, Manchester, UK. ⁹Cancer Research UK Beatson Institute, Glasgow, UK. ¹⁰Institute of Cancer Sciences, University of Glasgow, Glasgow, UK. ¹¹Present address: Department of Life Science, Manchester Metropolitan University, Manchester, UK. ✉e-mail: griff@mit.edu; Claus.jorgensen@manchester.ac.uk

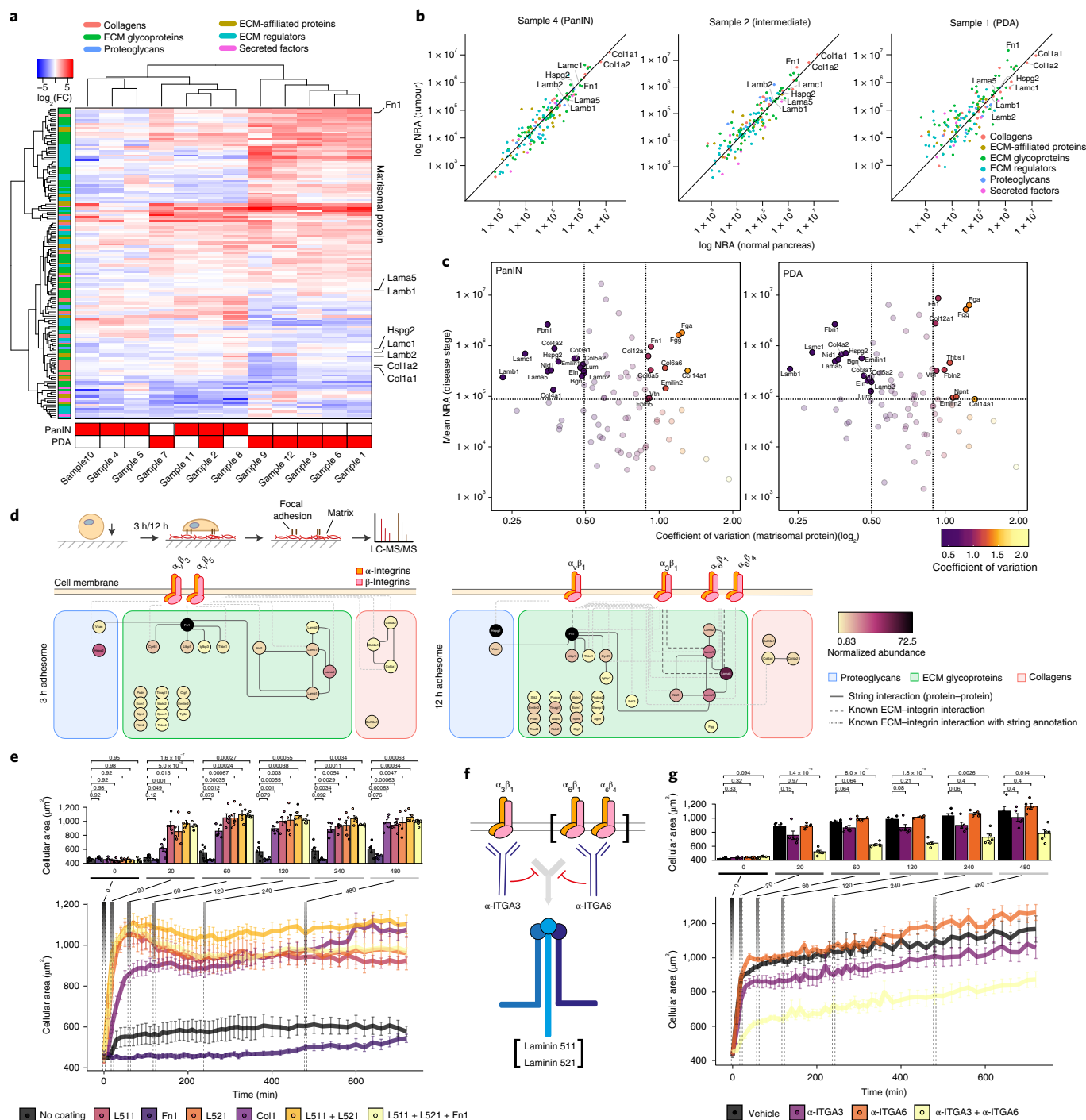


Fig. 1 | Defining adhesive requirements of PCCs. **a**, Hierarchical clustering of matrisomal protein relative abundances (compared to normal pancreas). Histological grade (bottom) and selected matrisomal proteins (right side) are shown. **b**, Normalized relative abundance (NRA) of matrisomal proteins from three representative samples (intermediate represents a mixed sample containing PanIN and PDA). The solid line represents similar abundance between samples. **c**, Scatter plot displaying the variance of core-matrisome proteins over mean NRA in PanIN (left) or PDA (right). Vertical lines represent the 25% quantile and 75% quantile coefficient of variation. Horizontal line indicates median abundance. **d**, Outline of integrin adhesion complex (IAC) isolation (top) and identified proteins (bottom). Interactions of selected proteins identified in IACs isolated from KPC-1s after 3 h (left) or 12 h (right) are shown. Proteins are colour-coded according to their relative abundance. **e**, Time-course of green fluorescent protein (GFP)-labelled human SUIT-2 PCCs spreading on indicated ECM proteins. **f**, Schematic outline of blocking antibodies targeting integrins $\alpha_6\beta_1$, $\alpha_6\beta_4$ or $\alpha_3\beta_1$. **g**, Effect of blocking antibodies on GFP-labelled SUIT-2 cells spreading on L511- and L521-coated dishes. **e, g**, Bar graphs show mean values ($n=5$), with each data point representing the median cellular area of >100 measured cells for indicated time points. In **e** and **g**, the number is the result of the statistical test (P -value) and the square brackets denote which samples are compared. Vertical dashed lines mark the time points selected for and visualized in the bar plots. Two-sided parametric Welch's t -test with Benjamini-Hochberg correction; error bars, s.e.m.

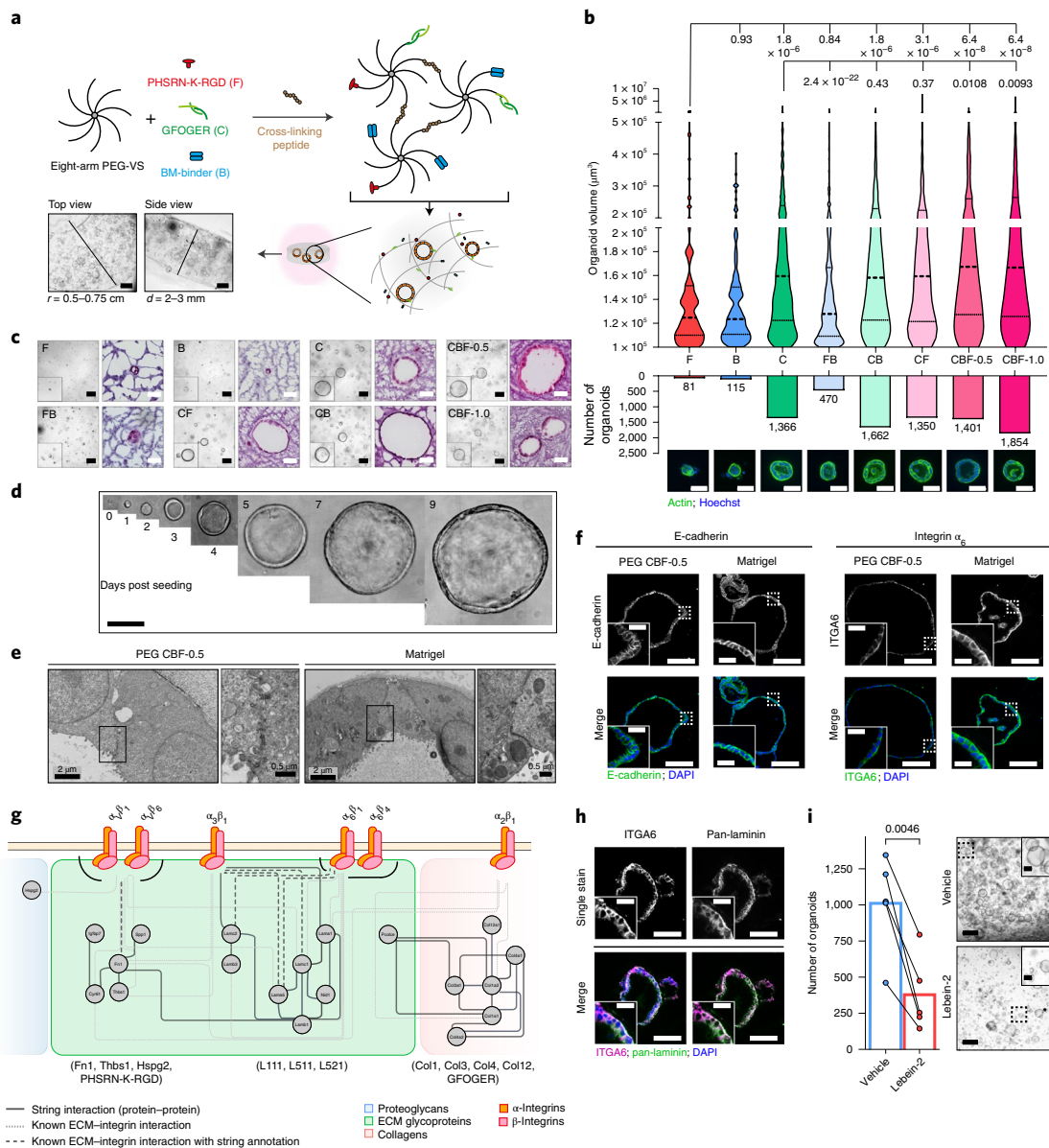


Fig. 2 | Optimizing PEG hydrogel composition for pancreatic organoids. **a**, Illustration of 3D PEG hydrogel scaffold crafting and organoid encapsulation. **b**, Image analysis of murine pancreatic cancer organoids (mPCOs) grown in 3D PEG hydrogels prepared with different adhesion-mimetic peptides as indicated. Violin plots display the volume distribution of individual organoids (top) (d4, $n=3$, two-tailed Wilcoxon test with Benjamini-Hochberg correction). Dashed bold line indicates median organoid volume. Total organoid number and representative images of analysed mPCOs are also shown (bottom). Scale bar, $50\text{ }\mu\text{m}$. **c**, Representative brightfield and H&E images of mPCOs in 3D PEG hydrogels using adhesion-mimetic peptides as indicated (d4, $n=3$). Brightfield scale bar, $200\text{ }\mu\text{m}$; H&E scale bar, $50\text{ }\mu\text{m}$. **d**, Representative brightfield images of mPCOs developing in 3D PEG CBF-0.5 hydrogels ($n=3$). Scale bar, $100\text{ }\mu\text{m}$. **e**, Representative electron microscopy images of mPCOs grown as indicated (d4). Black rectangles correspond to the higher magnification images to the right. Scale bar, $2\text{ }\mu\text{m}$; inset scale bar, 500 nm . Images are representative of minimum five organoids in each gel. **f**, Immunofluorescence (IF) images of mPCOs in PEG CBF-0.5 hydrogels or Matrigel. Dashed-outline rectangles correspond to the insets. Scale bar, $100\text{ }\mu\text{m}$; inset scale bar, $25\text{ }\mu\text{m}$. Images are representative of minimum five organoids in the respective gel (d4, $n=2$). **g**, Protein-protein interaction network of identified integrin-ECM interactions of mPCOs in 3D PEG CBF-0.5 hydrogels, highlighting main ECM ligands of identified integrins. **h**, Dual IF of pan-laminin and ITGA6 in mPCOs in 3D PEG CBF-0.5 hydrogels. Images are representative of minimum five organoids (d4, $n=2$). Scale bar, $100\text{ }\mu\text{m}$; inset scale bar, $25\text{ }\mu\text{m}$. **i**, Quantification (left) and representative brightfield images (right) of mPCOs in 3D PEG CBF-0.5 hydrogels with vehicle or lebein-2 (d4, $n=5$, paired parametric two-sided Welch's t -test). Individual replicates are linked. Dashed-outline rectangles correspond to the insets. In **b** and **i**, the number is the result of the statistical test (P -value) and the square brackets denote which samples are compared. Scale bar, $500\text{ }\mu\text{m}$; inset scale bar, $100\text{ }\mu\text{m}$. F, PHSRN-K-RGD; B, BM-binder; C, GFOGER; FB, CB and CF, combinations of indicated peptides; CBF-0.5 and CBF-1.0, combination of indicated peptides with PHSRN-K-RGD at 0.5 and 1 mM, respectively.

and tumour-bearing tissues, support co-culture of epithelial and stromal cells and facilitate growth and development of organoids directly from tissue samples.

Proteomic analysis of the tumour matrisome and functional validation of cellular adhesion requirements were used to develop a relevant PEG hydrogel scaffold. This system successfully

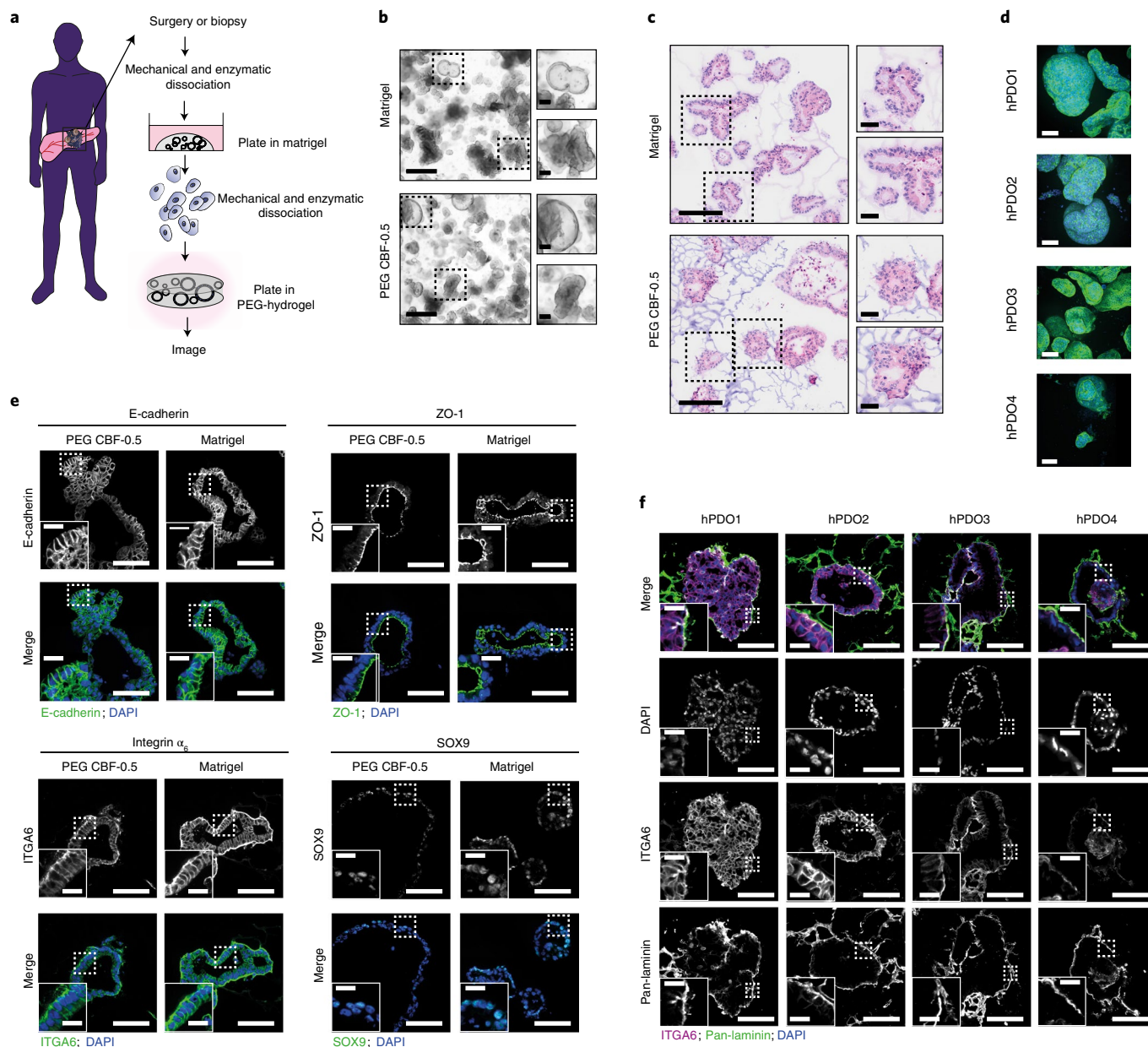


Fig. 3 | Formation of hPDOs in defined PEG matrices. **a**, Schematic of hPDO establishment. **b**, Representative brightfield images of hPDOs in 3D PEG CBF-0.5 hydrogels or Matrigel (d6). Images are representative of at least three independent experiments. Scale bar, 500 μm ; inset scale bar, 100 μm . **c**, H&E staining of organoids from **b**. Scale bar, 200 μm ; inset scale bar, 50 μm . **d**, Maximum intensity projection of hPDOs from four patients (hPDO1, hPDO2, hPDO3 and hPDO4) stained with Phalloidin and Hoechst to visualize organoid morphology and cellular structures. Images show representative morphology of organoids from each line. Scale bar, 200 μm . **e**, IF analysis of indicated markers in hPDO2 organoids grown in PEG CBF-0.5 hydrogels or Matrigel (d6, $n=2$). Scale bar, 100 μm ; inset scale bar, 25 μm . Images are representative of minimum five organoids. **f**, Dual IF for pan-laminin and ITGA6 in hPDOs grown in PEG CBF-0.5 hydrogels (d6, $n=2$). Images are representative of minimum five organoids. **e, f**, Scale bar, 100 μm ; inset scale bar, 25 μm . Dashed-outline rectangles in **b, c, e** and **f** correspond to insets.

replicates the entire stiffness range of normal and tumour-bearing tissue, supports growth of murine and human normal and cancerous organoids and essential stromal populations and is compatible with proteomic and single-cell analyses.

Results

Defining adhesive requirements of pancreatic cancer cells (PCCs). To reconstitute relevant ECM–receptor interactions within a custom-designed PEG environment, we first defined a matrisome reference set for *in vivo* pancreatic tissues²⁰. Normal pancreatic tissue (NP), pancreata with pancreatic intraepithelial neoplasia

(PanIN), known precursor lesions of PDA, and overt PDA from *Kras*^{G12D} and *TP53*^{R172H}-driven murine models were collected for analysis^{21–23} (Supplementary Fig. 1a). We confirmed the high reproducibility of the workflow by analysing ten normal pancreata by liquid chromatography with tandem mass spectrometry (LC–MS/MS) (Supplementary Fig. 1a–d) before analysing 12 tumour samples, which resulted in the identification and quantification of 147 matrisomal proteins, 83 of which predominantly exhibit structural functions (termed core matrisome) (Fig. 1a,b and Supplementary Figs. 2–5)²⁴. Analysis of relative protein abundances by hierarchical clustering segregated samples by their histological disease grade,

reflecting the evolving matrisomal remodelling that occurs during disease development (Fig. 1a,b and Supplementary Figs. 2 and 3). Comparison of adhesion-conferring matricellular protein levels with available PDA-matrisome datasets²⁵ highlighted several proteins, including fibronectin (FN), versican and laminin-332 (L332, $\alpha_3\beta_3\gamma_2$), that were upregulated in both human and murine PDA and correlate with patient outcome (Supplementary Fig. 4). By contrast, the BM proteins laminin 511 (L511, $\alpha_5\beta_1\gamma_1$) and laminin 521 (L521, $\alpha_5\beta_2\gamma_1$) and the type 1 and 4 collagens (for example, Col1a1, Col1a2, Col4a1 and Col4a2) were consistently highly abundant in both normal and disease-bearing pancreas (Supplementary Fig. 3b), with laminin 511 and 521 exhibiting minimal variation across samples (Fig. 1c and Supplementary Fig. 5c). Together, these findings highlight important and potentially complementary roles of individual matrisomal components, including FN, laminins (L322, L511 and L521) and collagens, throughout PDA development.

Integrins constitute a family of cellular ECM receptors that are fundamental to cellular adhesion and are commonly aberrantly expressed in malignant disease^{26–28}. To identify which receptors actively engage the ECM to form IACs, we seeded PCCs on FN-coated plates for 3 or 12 h and then analysed mature IACs by mass spectrometry^{29,30} (Fig. 1d and Supplementary Fig. 6). Interestingly, although PCCs were seeded on FN, the isolated IACs changed in composition from the canonical FN-binding integrins $\alpha_v\beta_3$ and $\alpha_v\beta_5$ after 3 h to laminin-binding integrins $\alpha_6\beta_1$, $\alpha_6\beta_4$ and $\alpha_3\beta_1$ after 12 h, concurrent with the deposition of laminin 521 and 511 (Fig. 1d and Supplementary Fig. 6). As this indicates that PCCs autonomously engineer the ECM to match their specific adhesion dependencies, we analysed the cell-derived matrix isolated from PCCs and normal pancreatic ductal epithelial cells (HPDE) by mass spectrometry. This analysis confirmed the deposition of a BM-rich ECM that included both L511 and L521 (Supplementary Fig. 7). Taken together, these data highlight a preference for L511- and L521-mediated tumour cell adhesion through α_6 - and α_3 -containing integrins³¹.

To test these observations functionally, cell culture dishes were pre-coated with selected ECM ligands that had been identified in the proteomic analysis, and the adhesion kinetics of relevant tumour and stromal cells were determined (Supplementary Fig. 8 and Supplementary Videos 1 and 2). Murine and human PCCs preferentially adhered to L511- and L521-pre-coated dishes, whereas pancreatic fibroblasts adhered to FN-coated dishes (Fig. 1e and Supplementary Figs. 9 and 10). PCCs adhered to collagen-1 in a cell-line-dependent manner, but consistently exhibited limited adhesion to FN-coated or non-coated culture dishes (Fig. 1e, Supplementary Figs. 9 and 10 and Supplementary Videos 3–9). Function-blocking antibodies directed against integrins α_3 and α_6

significantly reduced adhesion to L511- and 521-pre-coated dishes (Fig. 1f,g and Supplementary Fig. 10), confirming the importance of L511/L521-integrin $\alpha_{3/6}\beta_{1/4}$ -mediated PCC adhesion in vitro (Fig. 1g and Supplementary Fig. 10)^{32–34}.

Analysis of human PDA by immunohistochemistry (IHC) revealed that cytokeratin-positive PCCs express integrin subunits α_6 and β_4 , whereas β_1 and α_v are broadly expressed across both tumour and stromal cells. Integrins α_2 and α_3 appeared to be mostly inter-cellular. Lama5 staining was observed basal to cytokeratin-positive tumour cells (Supplementary Fig. 11), supporting relevant roles of L511-integrin and L521-integrin $\alpha_6\beta_1$ -, $\alpha_6\beta_4$ - and $\alpha_3\beta_1$ -mediated PCC adhesion as well as collagen- and FN-mediated adhesion via integrins $\alpha_v\beta_1$ and $\alpha_2\beta_1$, respectively, that may occur in vivo. Thus, we reasoned that inclusion of these adhesion cues would be needed to support epithelial and stromal cells within a synthetic hydrogel scaffold.

Optimizing PEG hydrogel composition for pancreatic organoids.

To model relevant cell-ECM interactions for pancreatic epithelial and stromal cells, we used an eight-arm PEG-based hydrogel system in which adhesion-linker pre-functionalized vinyl sulfone-activated PEG macromers (f-PEG-VS) are cross-linked via peptides sensitive to matrix metalloproteinase (MMP) to form the hydrogel scaffold (Fig. 2a)^{19,35}. To support cell adhesion, we incorporated the FN-mimetic peptide PHSRN-K-RGD (F) and the GFOGER peptide (C), mimicking both fibrillar and network forming collagen, as well as a BM-binding peptide to retain cell secreted matricellular proteins more broadly^{16,35–39}. All adhesion-conferring peptides were fully incorporated into the PEG scaffold with limited effect on the differential elastic gel modulus (Supplementary Fig. 12).

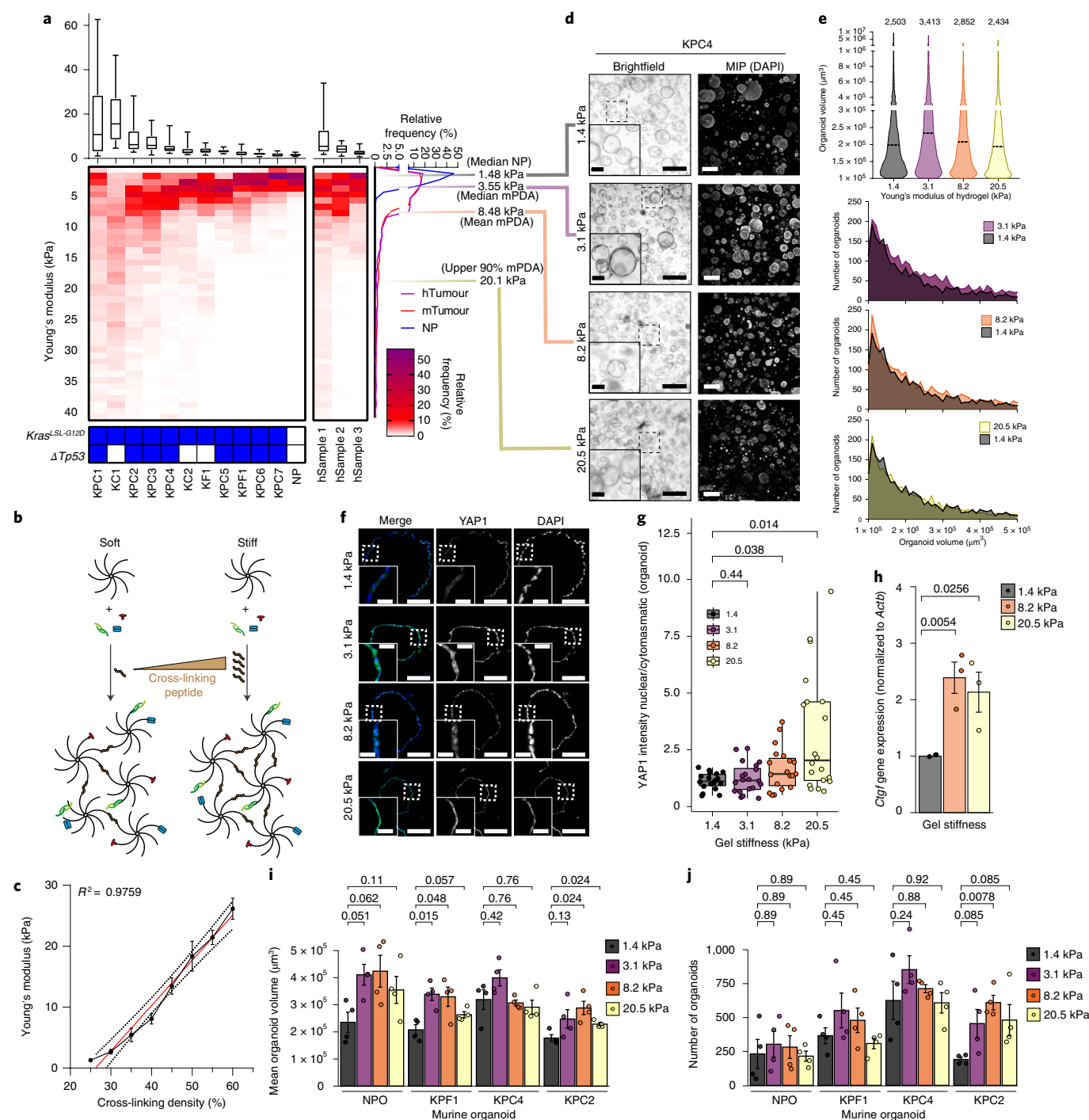
Established mPCOs were disaggregated into single cells and embedded into PEG-VS hydrogels prepared with different combinations of the adhesion-mimetic peptides (Fig. 2b,c). Whilst FN-mimicking and BM-binding peptides in isolation did not support organoid growth, the collagen-mimicking peptide supported expansion of mPCOs (Fig. 2b,c and Supplementary Fig. 13a). This contrasts with observations made using human colorectal and endometrial carcinoma organoid lines, which were sustained by FN-mimetic peptides^{17,19}, suggesting that synthetic matrices may need to be engineered to support adhesive requirements that are tissue and cell-type specific. Notably, the combination of all three peptide anchors (CBF) significantly enhanced the number and size of organoids compared to GFOGER (C) alone (Fig. 2b,c, Supplementary Fig. 13 and Supplementary Videos 10 and 11), demonstrating a complementary effect of the adhesion peptides on organoid formation and growth. As the matricellular analysis determined the relative in vivo abundance of collagen type I and

Fig. 4 | Recapitulating the stiffness range of PDA in PEG hydrogels. **a**, Box plot (top) and heat map (bottom) displaying stiffness frequency (Young's modulus) for murine (left, $n=11$ tumour, $n=3$ NP) and human (right, $n=3$) samples. Box plots represent individual measurements (>800 per sample). The bold line represents the median, boxes represent the 25th to 75th percentiles and whiskers indicate the 90% confidence interval. The genotype of murine samples is shown at the bottom of the panel. Cumulated relative stiffness frequency is shown on the right. Median stiffness for normal (grey) as well as median (purple), mean (orange) and upper 90% border (yellow) of murine cancerous samples. **b**, Illustration of how cross-linking density after PEG functionalization controls stiffness. **c**, AFM measurements of PEG CBF-0.5 hydrogels ($n=3$; error bars, s.e.m.). Linear regression (red) and 95% confidence interval shown (dashed line). **d**, Representative brightfield images (left) and maximum intensity projections of 4,6-diamidino-2-phenylindole (DAPI, right) from mPCOs grown at indicated stiffnesses (d4, $n=4$). Dashed-outline boxes correspond to insets. Scale bar, 500 μm ; inset scale bar, 100 μm (left). **e**, Violin plot of organoid volume (top) and frequency plots of numbers (bottom) from **d**. Dashed bold lines show median organoid volume. Number of analysed organoids shown above the plot. **f**, IF of yes-associated protein 1 (YAP1) and DAPI in mPCOs grown at indicated stiffness. IF images are representative of minimum five organoids ($n=2$). Dashed-outline boxes correspond to insets. Scale bar, 100 μm ; inset scale bar, 25 μm . **g**, Nuclear/cytoplasmic ratio of YAP1 in individual organoids from **f**. Mean shown as bold line. Two-sided parametric Welch's *t*-test used for 1.4, 3.1 or 8.2 kPa and two-sided non-parametric Wilcoxon test for 20.5 kPa with Benjamini-Hochberg correction. Bottom, middle and top lines of boxes show the 25th, 50th and 75th percentiles, respectively, and whiskers show 1.5 times the interquartile range from hinges. **h**, Normalized *Ctcf* expression in mPCOs grown at indicated stiffness ($n=3$; parametric Welch's *t*-test; error bars, s.e.m.). **i, j**, Mean organoid volumes (**i**) and numbers (**j**) of mPCOs grown at indicated stiffness ($n=4$; two-sided parametric Welch's *t*-test with Benjamini-Hochberg correction; error bars, s.e.m.). In **g–j**, the number is the result of the statistical test (*P*-value) and the square brackets denote which samples are compared.

FN at 2:1 in all pancreatic matrisome samples (Supplementary Fig. 13c), we used the CBF-0.5 hydrogel formulation for all subsequent studies.

Using this formulation, organoids matured and developed macroscopically visible spheres throughout the entire gel within 3 to 5 days of seeding (Fig. 2d and Supplementary Fig. 14a). In addition, organoids exhibited similar growth kinetics (Supplementary Fig. 14c) and established cellular architecture and polarity comparable to Matrigel when assessed by electron microscopy (Fig. 2e) or IF (Fig. 2f and Supplementary Fig. 14b). Finally, organoids from both normal- and tumour-bearing pancreas were supported at similar efficacy, suggesting that cancer cells retain adhesion dependencies that mirror their non-malignant history (Supplementary Fig. 14d).

To determine whether CBF-0.5 hydrogels support the formation of a relevant ECM, we determined the deposition of ECM proteins in the PEG culture systems by LC-MS/MS (Fig. 2g and Supplementary Fig. 15). This resulted in the identification of 104 matrisomal proteins, including laminin-521, laminin-511, type 1 collagen and FN, as well as the FN-binding integrins $\alpha_v\beta_1$ and $\alpha_v\beta_6$, the laminin-binding integrins $\alpha_3\beta_1$, $\alpha_6\beta_1$ and $\alpha_6\beta_3$ and the collagen-binding integrin $\alpha_2\beta_1$ (Supplementary Fig. 15). Using a dual-IF analysis, we confirmed the basolateral localization of integrin α_6 in close proximity to organoid-derived laminin deposits in the PEG CBF-0.5 gels (Fig. 2h). Importantly, laminin deposits were also identified in PEG hydrogels containing only the GFOGER and PHSRN-K-RGD peptides, indicating that the interactions



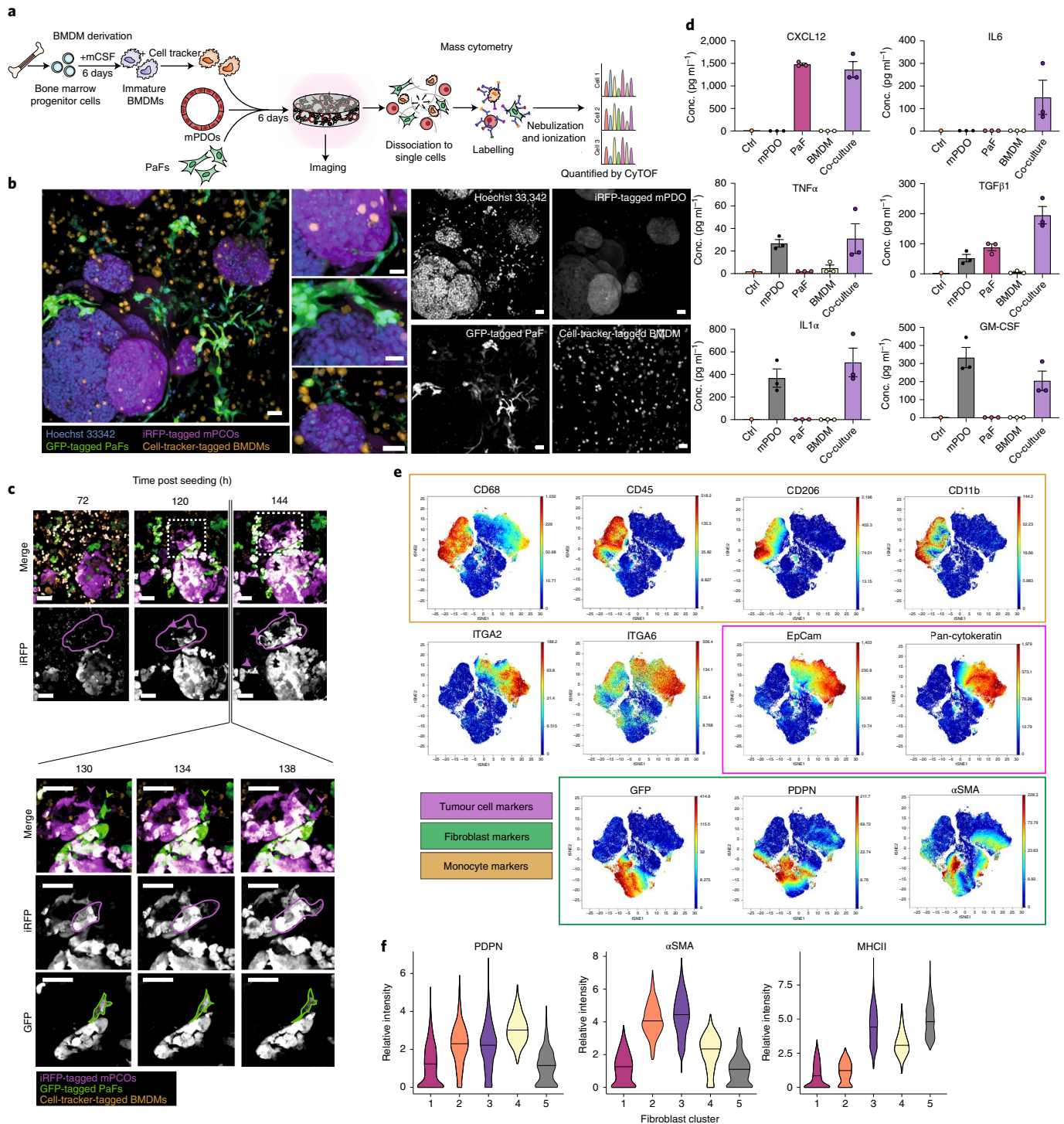


Fig. 5 | 3D PEG-VS CBF-0.5 gels support stromal co-cultures. **a**, Overview of co-culture in PEG-VS CBF-0.5 hydrogels. **b**, Representative image of co-cultures (d6). Scale bar, 70 μm ; images representative of three independent experiments. **c**, Representative images of co-cultures in 3D PEG-VS CBF-0.5 hydrogels at indicated time after seeding (top) and representative examples of fibroblasts and cancer cells (bottom). Images are representative of at least five individual regions centred around mPCOs. White boxes and purple outlines indicate regions of interest. Scale bar, 60 μm . **d**, Enzyme-linked immunosorbent assay (ELISA) of conditioned medium from mono- and co-cultures grown in PEG hydrogels for 6 days ($n=3$). Conc., concentration. Error bars, s.e.m. **e**, t-SNE visualization of mass cytometry analysis of PEG CBF-0.5 gel co-cultures overlaid with relative quantification of selected markers (d6, $n=2$). Integrin markers were not used in definition of t-SNE plots. Range of colorimetric scale is indicated for individual markers. **f**, Violin plots of selected markers for all detected fibroblast clusters. Bold line indicates median intensity of each marker and population.

between laminin and integrins α_6 and α_3 are functionally important for organoid growth (Supplementary Fig. 16a,b). To functionally verify this interaction, we treated mPCOs grown in PEG CBF-0.5

hydrogels with lebein-2, a disintegrin that selectively blocks the laminin-binding integrins $\alpha_3\beta_1$, $\alpha_6\beta_1$ and $\alpha_7\beta_1$ but does not target the collagen-binding integrins $\alpha_1\beta_1$ and $\alpha_2\beta_1$ (refs. 40–43). Lebein-2

interfered with adhesion of PCCs onto L511- and L521-coated dishes in vitro (Supplementary Fig. 16c,d) and significantly reduced mPCO formation and growth in PEG CBF-0.5 gels (Fig. 2i and Supplementary Fig. 16e–h). Together, these data demonstrate that relevant cell–ECM interactions are established in PEG hydrogels and that laminin–integrin interactions play a functionally important role for the growth of pancreatic cancer organoids. In conclusion, PEG CBF-0.5 hydrogels support the formation of complex cell–ECM interactions to enable the growth and polarization of pancreatic organoids with comparable efficacy to Matrigel.

Human pancreatic ductal organoid (hPDO) formation in defined PEG matrices. To determine whether the synthetic PEG CBF-0.5 hydrogel scaffold also supports expansion of human-patient-derived organoids, we seeded established hPDOs and tracked their growth and morphology (Fig. 3a). hPDOs were engrafted as fragments or single cells in PEG CBF-0.5 hydrogels, where they developed into fully mature spheres after 4–12 days of growth and exhibited similar morphology to hPDOs grown in Matrigel (Fig. 3b,c and Supplementary Fig. 17). Consistently with mPCOs, hPDOs exhibited a high degree of morphological heterogeneity in PEG and Matrigel culture conditions (Fig. 3c,d and Supplementary Fig. 17)⁴⁴. IF analysis confirmed that human organoids were polarized and retained expression of ZO-1, ITGA6, SOX9 and E-cadherin (Fig. 3e and Supplementary Fig. 17c–e). All hPDOs express integrin α_6 at the cell periphery, close to laminin deposits, indicating that laminin–integrin interactions are conserved in human pancreatic organoids (Fig. 3f). These data demonstrate that PEG CBF-0.5 hydrogels support murine and human pancreatic organoids growth in vitro.

Recapitulating the stiffness range of PDA in PEG hydrogels. Deregulated mechano-sensing is commonly observed in solid tumours, where a remodelled ECM promotes malignant traits^{45,46}. As synthetic hydrogel scaffolds can be configured to recapitulate tissue stiffening^{17,35}, we set out to determine whether the PEG hydrogel scaffold reliably replicates the stiffness ranges of normal and tumour-bearing pancreas.

To determine how tissue stiffness changes as normal healthy pancreas transitions into tumour-bearing tissue, we analysed 11 murine and 3 human fresh-frozen pancreatic cancerous samples by atomic force microscopy (AFM) and compared their stiffness profiles to those of three murine normal pancreata (Fig. 4a and Supplementary Figs. 18–20). Healthy murine pancreatic tissue exhibited a mean stiffness of 1.48 ± 0.3 kPa, while murine tumour-bearing tissue displayed a median stiffness of 3.55 kPa and a mean stiffness of 8.48 ± 2.2 kPa, with 90% of all measurements below ~ 20.1 kPa, confirming previous analyses^{46–48} (Fig. 4a and Supplementary Fig. 19). Similar stiffening was observed for the three human specimens (Fig. 4a and Supplementary Fig. 20). We confirmed these findings using second-harmonic generation (SHG) imaging for linearized collagen fibres, which are known to correlate with matrix stiffening⁴⁶ (Supplementary Fig. 21).

To model this environment in vitro, we tuned the stiffness of PEG CBF-0.5 hydrogels by increasing the molar ratio of the cross-linking peptide to the number of free vinyl sulfone (VS) arms (hereafter referred to as cross-linking density; Fig. 4b). We profiled the resulting hydrogels using AFM and confirmed the relative increase in stiffening by rheology (Supplementary Fig. 12e), demonstrating that the entire stiffness range from normal pancreas to PDA was recapitulated with high reproducibility (Fig. 4c).

To determine the effects of increased PEG hydrogel stiffening on organoid growth, we seeded murine organoids in hydrogels tuned to replicate the pathological stiffness of PDA (Fig. 4d,e and Supplementary Fig. 22). Organoids formed efficiently in hydrogels across the entire stiffness range, displayed elevated nuclear

translocation of YAP1 and increased Ctgf levels in stiffened hydrogels, consistent with engagement of mechano-signalling (Fig. 4f–h and Supplementary Fig. 23). To further profile differences in the cellular response to increased hydrogel stiffening, we seeded one murine normal pancreatic organoid (mPNO) and three mPCOs in PEG hydrogels tuned at disease-relevant stiffnesses. While all organoids exhibited a growth advantage when seeded in stiffened gels (Fig. 4i,j and Supplementary Fig. 22)⁴⁹, differences existed in the optimal stiffness for growth across the mPCOs, possibly reflecting the stiffness of the tumour from which the organoids were established. These data demonstrate that the PEG CBF-0.5 hydrogels present a suitable and reproducible model to study effects of tissue stiffening.

Modelling a heterocellular tumour microenvironment. To determine whether diverse stromal cell populations from pancreatic tumours are retained in PEG hydrogels, we collected and disaggregated tumours from orthotopically implanted mPCOs and embedded these in PEG CBF-0.5 hydrogels (Supplementary Fig. 24). Strikingly, stromal cell populations were readily detected by IHC for pan-CK, PDPN and CD45 after 8 days of culture, demonstrating the suitability of CBF-0.5 hydrogels for stromal co-cultures.

Next, we co-cultured mPCOs labelled with infrared fluorescent protein (iRFP), GFP-labelled murine pancreatic fibroblasts (PaFs) and cell-tracker-dye-labelled macrophages (BMDM) treated with murine bone-marrow-derived myeloid cells (BMDM) treated with macrophage colony stimulating factor 1 (csf-1), in PEG CBF-0.5 hydrogels (Fig. 5a). Fluorescent image, IHC and flow analysis after 6 days of culture validated that viable PaFs and macrophages were retained in the PEG CBF-0.5 hydrogels (Fig. 5b and Supplementary Fig. 25). Next, the cellular dynamics within co-cultures were examined by live imaging for 3 days. Dynamic migratory behaviour of both tumour and stromal cells was observed within the PEG CBF-0.5 hydrogels (Supplementary Fig. 26). For example, individual tumour cells in close proximity to fibroblasts exhibited invasive behaviour and migrated away from the organoid structure (Supplementary Fig. 26 and Supplementary Videos 12–15). Moreover, consistently with previous observations, we also observed that fibroblasts exhibited an elongated, mesenchymal morphology; this was especially apparent with fibroblasts proximal to tumour cells⁵⁰ (Fig. 5c and Supplementary Fig. 26).

To further interrogate the interaction of tumour and stromal cells, we determined the production of functionally important soluble signals (Fig. 5d). Several cell-specific signals such as GM-CSF, CXCL12 and IL1 α were identified across mono- and co-cultures, whereas other signals (IL6 and TGF β) increased robustly upon co-culture, demonstrating relevant tumour–stromal interactions (Fig. 5d). To further interrogate cellular phenotypes, we analysed co-cultures at single-cell resolution using cytometry by time of flight (CyTOF). Cells were liberated from PEG CBF-0.5 hydrogels after 6 days of co-culture and stained with antibodies directed against known markers of tumour cells, CAFs and macrophages, followed by analysis (Fig. 5e and Supplementary Fig. 27). Visualization using t-distributed stochastic neighbour embedding (t-SNE) distinguished cytokeratin- and EpCAM-positive epithelial mPCOs from the CD45^{pos}/CD68^{pos} BMDM-derived macrophages and GFP^{pos} fibroblasts, revealing phenotypic diversity across tumour and stromal cell populations. For example, fibroblasts expressed markers of known subsets, such as α SMA^{pos} myCAFs, MHCII^{pos} apCAFs and MHCII^{neg}/ α SMA^{neg} iCAFs (refs. ^{50,51}) (Fig. 5f and Supplementary Fig. 28). This demonstrates that stromal cell populations are readily incorporated with organoids in PEG hydrogels and exhibit signalling, phenotypic and morphological behaviour consistent with in vivo models. Thus, PEG CBF-0.5 hydrogels can be readily utilized for the study of pancreatic cancer within a functionally relevant stromal context.

Discussion

Contemporary organoid models that replicate physiochemical characteristics and stromal abnormalities of the tumour microenvironment are needed to improve basic and translational cancer biology.

Here we combined biochemical and functional analysis of cellular adhesion dependencies to inform the design of a synthetic PEG scaffold. Interactions between cell-derived laminin 511 and laminin 521 and integrin α_6 or α_3 subunits are recapitulated within a complex cell–ECM niche to support organoid growth. Moreover, PEG hydrogels recapitulate the entire stiffness range of murine and human pancreatic cancers and engage signalling consistent with mechano-sensing. Lastly, stromal cell populations such as pancreatic fibroblasts and bone-marrow-derived macrophages⁵¹ were readily co-cultured and fibroblasts express markers and display morphology consistent with adaptation of myCAF, iCAF and apCAF subsets⁵⁰, demonstrating that stromal cells acquire relevant phenotypes within these defined growth settings.

This rationally designed and easy-to-use PEG system provides exquisite growth control in a reproducible and defined manner to support future basic and translational studies of human and murine pancreatic organoids within a relevant microenvironment.

Online content

Any methods, additional references, Nature Research reporting summaries, source data, extended data, supplementary information, acknowledgements, peer review information; details of author contributions and competing interests; and statements of data and code availability are available at <https://doi.org/10.1038/s41563-021-01085-1>.

Received: 11 April 2020; Accepted: 21 July 2021;

Published online: 13 September 2021

References

- Egeblad, M., Nakasone, E. S. & Werb, Z. Tumors as organs: complex tissues that interface with the entire organism. *Dev. Cell* **18**, 884–901 (2010).
- Feig, C. et al. The pancreas cancer microenvironment. *Clin. Cancer Res.* **18**, 4266–4276 (2012).
- Sahai, E. et al. A framework for advancing our understanding of cancer-associated fibroblasts. *Nat. Rev. Cancer* **6**, 174–186 (2020).
- DeNardo, D. G. & Ruffell, B. Macrophages as regulators of tumour immunity and immunotherapy. *Nat. Rev. Immunol.* **7**, 369–382 (2019).
- Biankin, A. V. et al. Pancreatic cancer genomes reveal aberrations in axon guidance pathway genes. *Nature* **491**, 399–405 (2012).
- Miller, B. W. et al. Targeting the LOX/hypoxia axis reverses many of the features that make pancreatic cancer deadly: inhibition of LOX abrogates metastasis and enhances drug efficacy. *EMBO Mol. Med.* **7**, 1063–1076 (2015).
- Jiang, H. et al. Targeting focal adhesion kinase renders pancreatic cancers responsive to checkpoint immunotherapy. *Nat. Med.* **22**, 851–860 (2016).
- Shi, Y. et al. Targeting LIF-mediated paracrine interaction for pancreatic cancer therapy and monitoring. *Nature* **569**, 131–135 (2019).
- Sherman, M. H. et al. Vitamin D receptor-mediated stromal reprogramming suppresses pancreatitis and enhances pancreatic cancer therapy. *Cell* **159**, 80–93 (2014).
- Boj, S. F. et al. Organoid models of human and mouse ductal pancreatic cancer. *Cell* **160**, 324–338 (2015).
- Tuveson, D. & Clevers, H. Cancer modeling meets human organoid technology. *Science* **364**, 952–955 (2019).
- Drost, J. & Clevers, H. Organoids in cancer research. *Nat. Rev. Cancer* **18**, 407–418 (2018).
- Hughes, C. S., Postovit, L. M. & Lajoie, G. A. Matrigel: a complex protein mixture required for optimal growth of cell culture. *Proteomics* **10**, 1886–1890 (2010).
- Brassard, J. A. & Lutolf, M. P. Engineering stem cell self-organization to build better organoids. *Stem Cell* **24**, 860–876 (2019).
- Socovich, A. M. & Naba, A. The cancer matrisome: from comprehensive characterization to biomarker discovery. *Semin. Cell Dev. Biol.* **89**, 157–166 (2019).
- Cook, C. D. et al. Local remodeling of synthetic extracellular matrix microenvironments by co-cultured endometrial epithelial and stromal cells enables long-term dynamic physiological function. *Integr. Biol.* **9**, 271–289 (2017).
- Gjorevski, N. et al. Designer matrices for intestinal stem cell and organoid culture. *Nature* **539**, 560–564 (2016).
- Kratochvil, M. J. et al. Engineered materials for organoid systems. *Nat. Rev. Mater.* **4**, 606–622 (2019).
- Valdez, J. et al. On-demand dissolution of modular, synthetic extracellular matrix reveals local epithelial-stromal communication networks. *Biomaterials* **130**, 90–103 (2017).
- Naba, A., Clauser, K. R. & Hynes, R. O. Enrichment of extracellular matrix proteins from tissues and digestion into peptides for mass spectrometry analysis. *J. Vis. Exp.* **101**, e53057 (2015).
- Hingorani, S. R. et al. *Trp53^{R172H}* and *Kras^{G12D}* cooperate to promote chromosomal instability and widely metastatic pancreatic ductal adenocarcinoma in mice. *Cancer Cell* **7**, 469–483 (2005).
- Hruban, R. H. et al. Pathology of genetically engineered mouse models of pancreatic exocrine cancer: consensus report and recommendations. *Cancer Res.* **66**, 95–196 (2006).
- Schönhuber, N. et al. A next-generation dual-recombinase system for time- and host-specific targeting of pancreatic cancer. *Nat. Med.* **20**, 1340–1347 (2014).
- Naba, A. et al. The matrisome: in silico definition and in vivo characterization by proteomics of normal and tumor extracellular matrices. *Mol. Cell Proteom.* **11**, M111.014647 (2012).
- Tian, C. et al. Proteomic analyses of ECM during pancreatic ductal adenocarcinoma progression reveal different contributions by tumor and stromal cells. *Proc. Natl Acad. Sci. USA* **116**, 19609–19618 (2019).
- Horton, E. R. et al. Definition of a consensus integrin adhesome and its dynamics during adhesion complex assembly and disassembly. *Nat. Cell Biol.* **17**, 1577–1587 (2015).
- Humphries, J. D. Integrin ligands at a glance. *J. Cell. Sci.* **119**, 3901–3903 (2006).
- Hamidi, H. & Ivaska, J. Every step of the way: integrins in cancer progression and metastasis. *Nat. Rev. Cancer* **18**, 533–548 (2018).
- Jones, M. C. et al. Isolation of integrin-based adhesion complexes. *Curr. Protoc. Cell Biol.* **66**, 9.8.1–9.8.15 (2015).
- Robertson, J. et al. Defining the phospho-adhesome through the phosphoproteomic analysis of integrin signalling. *Nat. Commun.* **6**, 6265 (2015).
- Takizawa, M. et al. Mechanistic basis for the recognition of laminin-511 by $\alpha_6\beta_1$ integrin. *Sci. Adv.* **3**, e1701497 (2017).
- Samarelli, A. V. et al. Neuroligin 1 induces blood vessel maturation by cooperating with the α_6 integrin. *J. Biol. Chem.* **289**, 19466–19476 (2014).
- Aumailley, M., Timpl, R. & Sonnenberg, A. Antibody to integrin α_6 subunit specifically inhibits cell-binding to laminin fragment 8. *Exp. Cell Res.* **188**, 55–60 (1990).
- Lee, S. P. et al. Sickle cell adhesion to laminin: potential role for the α_5 chain. *Blood* **92**, 2951–2958 (1998).
- Hernandez-Gordillo, V. et al. Fully synthetic matrices for in vitro culture of primary human intestinal enteroids and endometrial organoids. *Biomaterials* **254**, 120125 (2020).
- Johnson, G. & Moore, S. W. Identification of a structural site on acetylcholinesterase that promotes neurite outgrowth and binds laminin-1 and collagen IV. *Biochem. Biophys. Res. Commun.* **319**, 448–455 (2004).
- Brown, A. et al. Engineering PEG-based hydrogels to foster efficient endothelial network formation in free-swelling and confined microenvironments. *Biomaterials* **243**, 119921 (2020).
- Knight, C. G. et al. The collagen-binding A-domains of integrins $\alpha_1\beta_1$ and $\alpha_2\beta_1$ recognize the same specific amino acid sequence, GFOGER, in native (triple-helical) collagens. *J. Biol. Chem.* **275**, 35–40 (2000).
- Kuhlman, W., Taniguchi, I., Griffith, L. G. & Mayes, A. M. Interplay between PEO tether length and ligand spacing governs cell spreading on RGD-modified PMMA-g-PEO comb copolymers. *Biomacromolecules* **8**, 3206–3213 (2007).
- Eble, J. A., Bruckner, P. & Mayer, U. Vipera lebetina venom contains two disintegrins inhibiting laminin-binding β_1 integrins. *J. Biol. Chem.* **278**, 26488–26496 (2003).
- Cavaco, A. C. M. et al. The interaction between laminin-332 and $\alpha_3\beta_1$ integrin determines differentiation and maintenance of CAFs, and supports invasion of pancreatic duct adenocarcinoma cells. *Cancers* **11**, 14–20 (2019).
- Gasmi, A. et al. Amino acid structure and characterization of a heterodimeric disintegrin from Vipera lebetina venom. *Biochim. Biophys. Acta* **1547**, 51–56 (2001).
- Arruda Macêdo, J. K., Fox, J. W. & de Souza Castro, M. Disintegrins from snake venoms and their applications in cancer research and therapy. *Curr. Protein Pept. Sci.* **16**, 532–548 (2015).
- Tiriach, H. et al. Organoid profiling identifies common responders to chemotherapy in pancreatic cancer. *Cancer Discov.* **8**, 1112–1129 (2018).
- Levental, K. R. et al. Matrix crosslinking forces tumor progression by enhancing integrin signaling. *Cell* **139**, 891–906 (2009).

46. Laklai, H. et al. Genotype tunes pancreatic ductal adenocarcinoma tissue tension to induce matricellular fibrosis and tumor progression. *Nat. Med.* **22**, 497–505 (2016).
47. Rice, A. J. et al. Matrix stiffness induces epithelial–mesenchymal transition and promotes chemoresistance in pancreatic cancer cells. *Oncogenesis* **6**, e352 (2019).
48. Rubiano, A. et al. Viscoelastic properties of human pancreatic tumors and in vitro constructs to mimic mechanical properties. *Acta Biomaterialia* **67**, 331–340 (2018).
49. Panciera, T. et al. Reprogramming normal cells into tumour precursors requires ECM stiffness and oncogene-mediated changes of cell mechanical properties. *Nat. Mater.* **19**, 797–806 (2020).
50. Öhlund, D. et al. Distinct populations of inflammatory fibroblasts and myofibroblasts in pancreatic cancer. *J. Exp. Med.* **214**, 579–596 (2017).
51. Elyada, E. et al. Cross-species single-cell analysis of pancreatic ductal adenocarcinoma reveals antigen-presenting cancer-associated fibroblasts. *Cancer Discov.* **9**, 1102–1123 (2019).

Publisher's note Springer Nature remains neutral with regard to jurisdictional claims in published maps and institutional affiliations.

© The Author(s), under exclusive licence to Springer Nature Limited 2021

Methods

Mouse models. KPC (*Kras^{LSL-G12D/Wt1}; Trp53^{LSL-R172H/Wt1}; Pdx-1-Cre*), KPFF (*Kras^{Frt-S-Frt-G12D/Wt1}; Trp53^{KO/Wt1}; Pdx-1-Flp*), KC (*Kras^{LSL-G12D/Wt1}; Pdx-1-Cre*) and KF (*Kras^{Frt-S-Frt-G12D/+}; Pdx-1-Flp*) animals have previously been described^{21,23,52}. Animals were bred in-house at CRUK Manchester (CRUK MI) or Beatson Institute (CRUK BI) under pathogen-free conditions. Mice were maintained in a purpose-built facility in a 12 h light–dark cycle at uniform temperature and humidity with continual access to food and water. The genotype of animals was confirmed by Transnetyx (Cordoba). For orthotopic tumour cell implantation studies, six-week-old female CD-1 nude animals were obtained from Charles River. All animal experiments were performed under a UK Home Office Licence and in accordance with the Animal (Scientific Procedures) Act of 1986 under project licence nos. 70/8745 and 70/8375 subject to review by the Animal Welfare and Ethical Review Body of Cancer Research UK Manchester Institute, University of Manchester (CRUK MI) and the University of Glasgow. Experiments are reported in accordance with Animal Research: Reporting of In Vivo Experiments (ARRIVE) 2.0 guidelines.

Patient samples. Research samples were obtained from the Manchester Cancer Research Centre (MCRC) Biobank with informed patient consent obtained prior to sample collection. The MCRC Biobank (ethics code 18/NW/0092) is licensed by the Human Tissue Authority (licence number 30004) and is ethically approved as a research tissue bank by the South Manchester Research Ethics Committee (Ref: 07/H1003/161+5). The role of the MCRC Biobank is to distribute samples. For more information see www.mcrc.manchester.ac.uk/Biobank/Ethics-and-Licensing.

Cell culture of murine and human PCC lines. Work with mammalian cancer cell lines and organoids was performed under sterile conditions. Cells were grown at 37 °C in 5% CO₂ and humidified air. Murine KPC-1 cells were obtained from Jennifer Morton at CRUK BI, UK; iKras cells were kindly shared by Ronald DePinho (MD Anderson Cancer Research Centre, TX, USA); KPC-43 cells were a kind gift from Kris Freese (CRUK MI); human SUIT-2 cells were obtained from ATCC and human H6c7 immortalized adult HPDE cells were obtained from Ming Tsao, University of Toronto, University Health Network, Toronto, Canada^{53,54}. All cells were confirmed mycoplasma free and cultured in Dulbecco's Modified Eagle Medium (DMEM, Thermo Fisher Scientific) supplemented with 10% v/v foetal bovine serum (FBS, Life Technologies) and 1x HyClone solution (Invitrogen), hereafter referred to as DMEM 10% v/v FBS. HPDE cells were grown in keratinocyte serum-free medium (SFM) supplemented with 0.2 ng ml⁻¹ EGF (Invitrogen), 30 µg ml⁻¹ bovine pituitary extract (Invitrogen, catalogue no. 17005042) and 1x HyClone solution. PCC lines or HPDEs were allowed to reach a maximum confluence of 80% and split using 0.25% v/v Trypsin-Versene (Invitrogen). iKras cells were cultured in DMEM 10% v/v FBS supplemented with 1 µg ml⁻¹ doxycycline (Sigma-Aldrich) at all times.

Establishment and culture of mPNOs or mPCOs. mPNOs were isolated from wild-type C57-Black6 pancreata or tumour-bearing KPC mice with histologically verified PDA^{10,55}. Tissues were minced (<0.5 mm in diameter) and enzymatically digested with 5 mg ml⁻¹ Collagenase-II (Thermo Fisher Scientific) in advanced DMEM F12 (Gibco) supplemented with 1x GlutaMax (Gibco), 0.1 M HEPES (Thermo Fisher Scientific) and 50 U of penicillin-streptomycin (Thermo Fisher Scientific), hereafter referred to as AdF base medium, for 45 min at 37 °C, with shaking (700 r.p.m.). Cells were spun, washed and seeded in 20 µl droplets of growth-factor reduced phenol-red- and LDEV-free Matrigel (Corning) in 24-well plates and cultured in AdF base medium supplemented with 1 mM N-acetyl cysteine (Sigma-Aldrich), 100 ng ml⁻¹ Wnt3a (R&D Systems), 100 ng ml⁻¹ Human Noggin (PeproTech), 100 ng ml⁻¹ FGF-10 (PeproTech), 10 mM nicotinamide (Sigma-Aldrich), 0.5 µM A83-01 (BioTechne), 500 ng ml⁻¹ R-Spondin 1 (R&D Systems) and 0.01 µM gastrin (Sigma-Aldrich), hereafter termed hPOCM. For mPNOs, EGF (Invitrogen) was added to the hPOCM to a final concentration of 50 ng ml⁻¹. Media were changed every 2 days to allow consistent mPCO growth. For passaging, following removal of the growth media, Matrigel domes were depolymerized in ice-cold PBS. mPNOs were mechanically dissociated into fragments using a 200 µl pipette tip and replated at a 1:6 split into new 20 µl Matrigel droplets. Frozen organoid stocks were established by mixing dissociated organoid fragments with Recovery Cell Culture Freezing Medium (RCFM, Gibco) followed by gentle cryopreservation. Organoids were thawed by rapidly warming cryotubes and following washing mPCOs twice in warm AdF base medium, mPCOs were seeded in 20 µl droplets of Matrigel. Growth media were replaced every other day for the first 2 days of culture following thawing, and mPCOs were passaged at least once before usage for experimental procedures.

Culture and establishment of hPDOs. hPDOs were established from fine-needle biopsy or resected pancreatic cancer specimens¹⁰. Tumour tissue was minced and enzymatically digested with 5 mg ml⁻¹ Collagenase-II (Thermo Fisher Scientific) in AdF base medium for 45 min at 37 °C, with shaking (700 r.p.m.). Upon removal of red blood cells using red blood cell lysis buffer (Merck), cells were spun, washed and seeded in 20 µl droplets of Matrigel and grown in hPOCM. For passaging, following removal of the growth media, Matrigel domes were depolymerized in

ice-cold PBS. hPDOs were mechanically dissociated into fragments using a 200 µl pipette tip and replated at a 1:2 split into new 20 µl Matrigel droplets. Frozen organoid stocks were established by mixing dissociated organoid fragments with RCFM followed by gentle cryopreservation. Organoids were rapidly thawed and washed twice in warm AdF base medium. hPDOs were seeded in 20 µl droplets of Matrigel in enriched hPOCM (enrichment consisted of addition of 50 ng ml⁻¹ EGF (Invitrogen) and increasing concentrations of Wnt3a (200 ng ml⁻¹) and R-Spondin 1 (1 µg ml⁻¹)). hPDOs were passaged at least once before usage for experimental procedures.

Adhesion assays. For PCC or pancreatic fibroblast (PaF) adhesion assays, fluorophore-labelled PCCs or PaFs were prepared in single-cell suspension. Cells were then extensively washed in DMEM without FBS, and 2,000 single cells were seeded in DMEM without FBS onto pre-coated wells of a glass-bottom 96-well plate (CellCarrier Ultra, PerkinElmer). For coating, 96-well plates were incubated with ECM ligand overnight at 4 °C in 70 µl PBS containing magnesium and calcium (PBS⁺⁺, Thermo Fisher Scientific) followed by another incubation for 30 min at room temperature. Wells were pre-coated with ECM ligands: rat-tail collagen-1 (0.1 mg ml⁻¹, Corning, catalogue no. 35429), FN from bovine plasma (5 µg ml⁻¹, Sigma-Aldrich, F1141), laminin 10 (5 µg ml⁻¹, Biolamina, LN511), laminin 11 (5 µg ml⁻¹, Biolamina, LN521) or combinations of those proteins. For collagen coating, the collagen-1 solution was carefully neutralized with 1 N NaOH (Sigma-Aldrich) according to the manufacturer's instructions in ultrapure water supplemented with 10x PBS. ECM ligands were then removed and wells were washed twice with PBS. Upon seeding of the cells, the plate was spun at 50 g for 1 min to collect cells at the bottom of the culture plate and imaging started immediately. Live imaging was conducted using confocal fluorescence high-content screening via the PerkinElmer Opera Phenix (PerkinElmer), a confocal spinning disk four-laser (405 nm 50 mW, 488 nm 50 mW, 591 nm 50 mW and 640 nm 50 mW) fixed light path system, with a range of emission filters (435–550 nm, 435–480 nm, 500–550 nm, 570–630 nm and 650–760 nm) and environmental control set to 37 °C, 5% CO₂ throughout the entire experiment. Four Zyla sCMOS cameras (2,160 pixels × 2,160 pixels, 6.5 µm pixel size (Andor)) are set up for each dedicated light path. A Zeiss W Plan-Apochromat ×20 water objective (numerical aperture (NA) 1.0, working distance (WD) 1.17 mm) was used. Prior to the time-course imaging, the vertical position of the z-stack was adjusted, and a z-stack of ±6 µm around the cell-adhesion plane was obtained for each of nine fields of view in each well. Images were obtained every 10 min for each well and condition for the first 6 h of the experiment, followed by imaging every 20 min till 12 h post seeding. For blocking studies on human SUIT-2 cells, prior to seeding, 37,500 single cells were pre-incubated for 30 min at 37 °C, 5% CO₂, with blocking antibodies anti-Itga6 (10 µg ml⁻¹, Merck Millipore, catalogue no. MAB1378, clone NK1-GoH3) or anti-Itga3 (10 µg ml⁻¹, Thermo Fisher Scientific, catalogue no. 17-0494042, clone P1B5) or combinations in 250 µl of DMEM. For blocking studies, 15,000 single cells were seeded in 100 µl DMEM. PBS was used as vehicle control. For lebein-2 adhesion assays, 2,000 murine KPC-1 cells were seeded onto surfaces pre-coated with laminin 511 or 521 (5 µg ml⁻¹ each) in the presence of either 10, 20 or 40 µg ml⁻¹ lebein-2 or a vehicle control in 100 µl DMEM; 50 mM HEPES, 150 mM NaCl solution (pH 7.4) was used as vehicle control. Following acquisition, cell masks were detected from the fluorophore channel and the cellular area was calculated using the Harmony software suite (PerkinElmer, v.4.8). Minimum 100 cells were analysed for each condition. Representative images of cells from adhesion assays were exported using the Harmony software suite (PerkinElmer, v.4.8) in 'highlighted' settings with gamma set to 2.3 to aid the visual interpretation of the images.

PEG, synthetic peptides and hydrogel formulation. Eight-arm 20 kDa PEG-VS macromers were purchased from JenKEM Technology. All peptides were custom synthesized and purified (> 95%) by AppTec or Genscript. The following peptides were used in this study:^{16,19} MMP-CL, a diethyl cross-linking peptide containing an MMP- and sortase-sensitive recognition site, (Ac) GCRD-LPRTG-GPQGIWQG-DRCG(Am); PHSRN-K-RGD, an FN-derived adhesion peptide containing the PHSRN synergy site and the RGD motif from the 9th and 10th FN type III repeat, respectively, in a branched assembly, (Ac) PHSRNGGGK-[GGGERCG(Ac)]-GGRGDSPPY(Am) (ref. 39), labelled with the single letter 'F' in the gels; GFOGER, a triple-helical collagen-I-derived adhesion peptide, (Ac)GGYGGGPG(GPP)₂GFOGER(GPP)₂GPC(Am)¹⁷, labelled with the letter 'C' in the gels; and BM-binder, a peptide with high affinity for BM-derived proteins, specifically collagen type IV and laminin, (Ac) GCRE-ISAFLGIPFAEPPMGPRRFLPPEPKK(Am)³⁹, labelled with the letter 'B' in the gels. All peptides were reconstituted in ultrapure water (Thermo Fisher Scientific) at a concentration of 20 mM for all adhesion-mimetic and BM-binding peptides and 50 mM for the MMP-CL cross-linker. The concentration of free thiols was determined using the Ellman's Reagent (Thermo Fisher Scientific) according to the manufacturer's instructions using an L-cysteine standard (Thermo Fisher Scientific).

Encapsulation of mPCOs as mono- or co-cultures with PaFs and BMDMs in PEG-VS hydrogels. Synthetic hydrogels were fabricated as described previously¹⁹.

In brief, hydrogels were crafted using Michael-type reaction chemistry inside a 1 ml syringe (BD) modified by removal of the tip. All hydrogels were prepared by reacting 1.5 mg of an eight-arm 20kDa-PEG-VS macromer (2.4 mM PEG-VS (19.7 mM VS) at 98% substitution) with the corresponding thiol-containing (–SH) adhesion and/or BM-binding peptides, in 1x PBS/1 M HEPES (pH 7.8, Gibco). For adhesion screening experiments, we prepared a series of peptide-functionalized PEG macromers (fPEG-VS) as follows: for hydrogels C, F and B, we used 1 mM of GFOGER, 1 mM of PHSRN-K-RGDS and 1 mM of BM-binder, respectively. For hydrogels CF, CB and FB, we used a combination of two different peptides (GFOGER, PHSRN-K-RGD or BM-binder) at 1 mM each, for a final peptide concentration of 2 mM in each gel formulation. The CBF-0.5 hydrogel was made using 1 mM of GFOGER, 1 mM PHSRN-K-RGDS and 0.5 mM BM-binder. Finally, for the CBF-1.0, we combined 1 mM of GFOGER, 1 mM PHSRN-K-RGDS and 1 mM BM-binder. The resulting fPEG-VS solutions were incubated for 30 min at 37 °C in a humidified incubator to allow complete functionalization of the PEG-VS arms.

Organoids were retrieved from Matrigel, dissociated into single cells by addition of 1x TrypLE Express (Gibco) for 10 min at 37 °C, diluted in AdF base medium and resuspended in minimal volume of AdF base. GFP-PaF and BMDM cells were collected using Accutase (Thermo Fisher Scientific) for 5 min at 37 °C and diluted in DMEM v/v 10% FBS followed by resuspension in a minimal volume of AdF base. The fPEG-VS solution was mixed with a cell suspension containing 10,000 PDO cells μl^{-1} to give a final concentration of 1,000 cells μl^{-1} hydrogel for monoculture experiments. For co-culture experiments PaFs and BMDMs were each included at 50,000 cells μl^{-1} in cell suspension for a final concentration of 5,000 cells μl^{-1} hydrogel, generating a 1:5:5 ratio of PDO:PaF:BMDM. The fPEG-VS-cell mixture was polymerized by addition of MMP-CL cross-linker followed by incubation for 45 min at 37 °C in a humidified incubator. CBF-0.5 hydrogels were prepared with the following cross-linker densities: 25% (4.95 mM), 30% (5.92 mM), 35% (6.89 mM), 40% (7.88 mM), 45% (8.86 mM), 50% (9.85 mM), 55% (10.83 mM) and 60% (11.82 mM). Polymerized gels were extracted from the modified syringes using a scalpel and dispersed into 24-well plates filled with 1 ml of hPOCM for monoculture or m-hPOCM for co-culture experiments. Care was taken to fully submerge the gels in the growth media. Cultures were maintained in a humidified incubator at 37 °C, 5.0% CO₂, with media changes every 2 days.

IF and IHC of hydrogels. Synthetic hydrogels or Matrigel plugs were embedded in O.C.T. medium (TissueTek) and snap-frozen in a dry ice/isopentane (Fisher Scientific, catalogue no. 10407010) mix for 5–10 min and prepared as 7 μm -thick sections using the cryotome instrument (Thermo Fisher Scientific Cryostat NX70). For IF, samples were then fixed for 15 min in 4% paraformaldehyde (PFA) (Thermo Fisher Scientific) and washed in PBS followed by blocking with 10% casein solution (Vector Labs, catalogue no. SP-5020). For E-cadherin and SOX9, cells were fixed in 1:1 acetone/methanol for 15 min at 4 °C. Primary rabbit anti-ZO-1 (1:100, Invitrogen, catalogue no. 61–7300); rat anti-CD49f (1:500, Merck Millipore, catalogue no. MAB1378, clone NK1-GoH3); rabbit anti-E-cadherin (1:100, Cell Signaling Technology, catalogue no. 3195, clone 24E10); rabbit anti-SOX9 (1:300, Merck Millipore, catalogue no. AB5535), rabbit anti-laminin (1:50, Abcam, catalogue no. ab11575) and rabbit anti-YAP1 (1:100, Cell Signaling Technology, catalogue no. 4912S) antibodies diluted in phosphate buffered saline + 0.1% Tween (PBST) were incubated for 1 h at room temperature. For anti-YAP1, samples were stained overnight at 4 °C. After washing in PBST three times for 5 min each, samples were incubated with Alexa-488 conjugated donkey anti-Rabbit (1:400, Invitrogen, catalogue no. A21206) or Alexa-488 conjugated donkey anti-Rat (1:400, Invitrogen, catalogue no. A21208) secondary for 30 min at room temperature. For dual-staining, samples were incubated with Alexa-488 conjugated donkey anti-Rabbit (1:400, Invitrogen, catalogue no. A21206) and Alexa-647 conjugated goat anti-Rat (1:400, Invitrogen, catalogue no. A21247) antibodies. Following washing in PBST, cells were incubated for 10 min at room temperature with DAPI (1:2,000, Thermo Fisher Scientific, catalogue no. 62248). Slides were cover-slipped using Prolong Gold Antifade (Thermo Fisher Scientific, catalogue no. P36930) and imaged in confocal fluorescence on the Olympus VS-120 instrument (Olympus) using a $\times 20$ objective following pre-scanning using a $\times 4$ objective to account for the focus position. Representative organoids were selected and exported from whole scanned slides using the QuPath software⁵⁶ (QuPath v.0.2.3) to Tagged Image File Format (TIFF). To aid visual interpretation of the data, images were scaled and care was taken to apply the same scaling for comparative samples (Supplementary Data 2 and 3). For quantification, images were exported without compression or rendering to the TIFF format. Quantification of IF staining was conducted on exported ROIs in the open-source Fiji software suite (v.1.52e, NIH)⁵⁷. For YAP1 quantification, staining intensities were exported using the plot profile function in Fiji from a segmented line (width = 40 pixels) drawn around the periphery of the organoid of interest without any alteration. DAPI signal was normalized by maximum intensity for each organoid and YAP1 intensities localized in gated nuclear regions (normalized DAPI ≥ 0.25 ; threshold validated by visual confirmation) were divided by intensities in cytoplasmic regions for each organoid. At least 20 organoids were quantified from three independent stainings. For pan-laminin deposit quantification, images were converted to 8-bit and a common threshold (10–255) was applied that was kept constant between all samples and measurements in Fiji. Organoid area was estimated using equation

(1), where d_1 and d_2 are the organoid's horizontal or vertical extensions respectively in R (v.4.0.0) as measured using Fiji.

$$A = \frac{d_1}{2} \times \frac{d_2}{2} \times \pi \quad (1)$$

For IHC, hydrogels were embedded in O.C.T., snap-frozen and sectioned at 7 μm . Sections were fixed for 15 min in 4% PFA at room temperature and washed in PBS. For podoplanin staining, cells were fixed in 1:1 acetone/methanol for 15 min at 4 °C. Endogenous peroxidase was blocked using 3% H₂O₂ in PBST for 10 min at room temperature followed by two PBST washes for 5 \times 2 minutes each. Non-specific antibody binding was blocked with 10% casein for 20 min at room temperature. Cells were then stained using primary rabbit anti-F4/80 (1:100, Cell Signaling Technology, catalogue no. 70076), rabbit anti-Pan-CK (1:100, Abcam, catalogue no. ab9377), rat anti-CD45 (1:100, BD Biosciences, catalogue no. 550539, clone 30-F11) or rabbit anti-Podoplanin (1:500, Thermo Fisher Scientific, catalogue no. MA5-29742) antibodies diluted in PBST for 1 h at room temperature. Following extensive washing, cells were stained with HRP conjugated goat anti-Rabbit secondary antibody (RTU, Dako, catalogue no. K4003) or HRP conjugated goat anti-Rat secondary antibody (RTU, Vector Laboratories, catalogue no. MP-7444) for 30 min at room temperature. Liquid DAB+ (Dako, catalogue no. K3468) chromogen was applied for 5 min at room temperature followed by counterstaining in Gills I haematoxylin (Thermo Fisher Scientific, catalogue no. 6765006) for 30 s. After mounting in Pertex mounting medium (CellPath, catalogue no. SEA-0100-00A), slides were scanned on the Leica SCN400 (Leica Microsystems), using a $\times 20$ objective lens under brightfield using the Leica LAS software to control the hardware and export the data to TIFF format. Raw Leica format files are initially stored onto a Synology RAID system and the exported to a read-only central storage solution to ensure data integrity.

High-content image analysis of hydrogels. Hydrogels were washed in PBS, and following fixation for 30 min in 4% PFA and permeabilization for 15 min in 0.1% Triton X-100 and blocking in 2% BSA, 1% FBS in PBS at room temperature for 4–12 h, cells were incubated with Alexa-488 conjugated Phalloidin (1:200, Thermo Fisher Scientific) and Hoechst (1:200, Thermo) in blocking buffer overnight at 4 °C with gentle shaking. After extensive washing in PBS, hydrogel plugs were transferred into glass-bottom 24-well CellCarrier imaging plates (PerkinElmer) and imaged using confocal fluorescence high-content screening via the Opera Phenix (PerkinElmer Waltham, MA), a confocal spinning disk four-laser system (405 nm 50 mW, 488 nm 50 mW, 591 nm 50 mW, 640 nm 50 mW) with a range of emission filters (435–550 nm, 435–480 nm, 500–550 nm, 570–630 nm, 650–760 nm). Four Zyla sCMOS cameras (2,160 pixels \times 2,160 pixels, 6.5 μm pixel size (Andor)) were set up for each dedicated light path. A Zeiss EC Plan Neofluar $\times 10$ air objective (NA 0.3, WD 5.2 mm) or Zeiss W Plan-Apochromat $\times 20$ water objective (NA 1.0, WD 1.17 mm) were used as indicated. Pre-scan directed z-stack acquisition of each individual sphere within the gel plug was used for monoculture experiments. For quantitative mono and co-culture experiments z-stacks were taken throughout the gel plug and organoids were counted using Harmony 4.8 (PerkinElmer) software suite in 3D rendered images. Representative images were exported from Harmony 4.8 in the portable network graphic format with scaling equally applied to all conditions.

Lebein-2 isolation and purification. Lebeins were isolated from the venom of *Macrovipera lebetina obtusa* (Latoxan, catalogue no. L1126) as described previously⁴⁰. In brief, upon gel filtration of the venom proteins on a Sepharose 6 column (GE Healthcare) in 20 mM sodium phosphate, pH 6.5, 50 mM sodium chloride and 1 mM EDTA, the relevant fractions were pooled, diluted with 10 mM MES (pH 5.7) and loaded onto a Mono S column (GE Healthcare). Lebein-2 was then eluted in a linear sodium chloride gradient from 80 to 140 mM and further purified on a C8 reversed-phase column (Nucleosil, Macherey Nagel) in a linear gradient from 0.1% trifluoroacetic acid in water to 80% acetonitrile in 0.08% trifluoroacetic acid in water. After lyophilization, the lebeins were dissolved in a 50 mM HEPES, 150 mM NaCl solution (pH 7.4) and kept at –80 °C until use. Lebein-2 charges used in this study were validated for effectiveness in adhesion assays.

Comparison of growth between Matrigel and PEG CBF-0.5 hydrogels and lebein-2 treatment. To evaluate murine PDO (mPDO) growth rate, single-cell suspensions of iRFP-labelled mPDOs were generated and encapsulated in PEG CBF-0.5 or Matrigel at 1,000 cells per μl hydrogel as previously described. Growth was assessed by measuring iRFP signal using Odyssey imaging system (Licor). For lebein-2 treatment assays, mPCOs were incorporated in PEG CBF-0.5 hydrogels as previously described at a concentration of 1,000 cells per μl hydrogel. Upon gelation, cells grown in hPCOM supplemented with 40 $\mu\text{g ml}^{-1}$ lebein-2 or a vehicle control. Media were half-replenished every day and new lebein-2 was added to the cells to maintain the inhibition. A 50 mM HEPES, 150 mM NaCl solution (pH 7.4) was used as vehicle control.

Reverse transcription-quantitative PCR (RT-qPCR). RNA of murine organoids grown in synthetic gels was isolated using the TRIzol reagent (Invitrogen)

according to the manufacturer's instructions. In brief, organoids were washed twice with PBS for 5 min at room temperature with shaking, and gels were thereafter snap-frozen and minced using a mortar and pestle in the presence of liquid nitrogen. Thereafter, 1.5 µg of RNA were reverse-transcribed using the RevertAid H Minus Reverse Transcriptase (Thermo Fisher Scientific), Random Hexamers (Thermo Fisher Scientific) and SoFast EvaGreen Supermix (Bio-Rad, catalogue no. 1725201) according to the manufacturer's instructions. The qPCR was conducted on complementary DNAs using the QuantStudio real-time PCR system (Thermo Fisher Scientific) and analysed using the QuantStudio Design & Analysis software (Applied Biosystems by Thermo Fisher Scientific, v.1.5.1, 2016). Expression values were obtained by applying the $2^{-\Delta\Delta Ct}$ method²⁹ and normalized to β -actin (*Actb*) in R (v.4.0.0). The selected primers are designed to amplify short fragments (99 to 121 base pairs) and validated to obtain optimal PCR efficiency between 85% and 115% efficiency. The list of primers and their validation parameters are described in Supplementary Table 1.

AFM. Tissue pieces isolated from the diseased portion of the pancreas and spanning the entire width of the tumour (for murine samples, $d = 1-1.5$ cm; $d = 0.5-1$ cm for human samples) were embedded in O.C.T. medium and snap-frozen on dry ice submerged in isopentane (Sigma-Aldrich). Sections 14 µm thick were cryosectioned from the frozen tissue blocks and stored at -20°C on glass slides (Superfrost Plus, Thermo Fisher Scientific) until required for AFM. Prior to use, sections were brought up to room temperature and rested for approximately 30 min to allow the sections to fully adhere to the glass slide. Following this, the sections were washed with copious amounts of ultrapure water to ensure complete removal of O.C.T. Sections were then air-dried overnight at room temperature. Each section was then rehydrated in ultrapure water for at least 10 min at room temperature immediately before data acquisition. AFM indentations were acquired using a Bruker Catalyst with a Nanoscope V controller (Bruker UK Ltd., Coventry UK) operating under Nanoscope software (v.4.8). The system was mounted on a Nikon Eclipse Ti-U inverted optical microscope (Nikon Instruments) equipped with a Hamamatsu ORCA-05G camera. For tissue sample indentations, 5 µm diameter gold colloid spheres mounted on cantilevers with a nominal spring constant of 0.1 N m^{-1} were used (CP-qp-CONT-Au-B, sQube). Cantilevers were calibrated before each experiment using the thermal oscillation method in air. For each tissue sample, force measurements were acquired from nine areas distributed over representative stromal and epithelial areas (as determined from an adjacent H&E stained section). In each area, data were obtained from 100 individual indentations, evenly spaced over a $25\text{ }\mu\text{m}^2$ area, with a ramp size of 4–6 µm and a maximal indentation depth (trigger threshold) of 40 nm ($<0.5\%$ of tissue sample depth). For biophysical profiling of hydrogels, gels were prepared 24 h before analysis. First, 20 µl of gel were pipetted onto pre-cleaned poly-L-lysine precoated glass slides (Thermo Fisher Scientific) and allowed to polymerize at 37°C for 40 min. Gels were then immersed in PBS and stored overnight at 37°C . Finally, the gels were washed twice in PBS before AFM measurements. For each PEG gel, ten force maps were obtained consisting of 25 individual indentations evenly acquired over $25\text{ }\mu\text{m}^2$. Data analysis for both the tissue samples and the gels was performed using the Bruker NanoScope Analysis software suite v.4.8 after baseline correction. The Hertz model was used to determine the elastic properties of the sample (equation (2)), with F being the force, E being Young's modulus, ν being the Poisson's ratio, R being the radius of the indenter and δ being the indentation. The adhesion force was not included, and maximal and minimal force fit boundaries of 80% and 20%, respectively, of the extension curve were used during all calculations. Values exceeding a Young's modulus of $x = \mu \pm 2\sigma$ (where x is any one calculated modulus value, μ is the mean of the calculated moduli values and σ is standard deviation) within each force map were removed from the analysis. A Poisson's ratio of 0.5 was assumed during calculations of the Young's moduli.

$$F = \frac{4}{3} \times \frac{E}{(1 - \nu^2)} \times \sqrt{R} \times \delta^{\frac{3}{2}} \quad (2)$$

IAC isolation. IACs of PCCs were isolated as previously described²⁹. In brief, for each condition and cell line, six dishes with a 10 cm diameter were coated with $10\text{ }\mu\text{g ml}^{-1}$ FN (Sigma-Aldrich, catalogue no. F1141) in PBS containing calcium and magnesium (PBS++; Thermo Fisher Scientific) to stimulate FN-mediated adhesion. PCCs were cultured and passaged and single cells seeded onto each FN-coated 10 cm dish in 5 ml of DMEM 10% (v/v) FBS. Following incubation at 37°C for either 3 h or overnight, the media were removed, and cells were washed twice with pre-warmed DMEM-HEPES (Sigma-Aldrich) to remove all non-adherent cells. IACs were then cross-linked by adding a 6 mM dimethyl 3,3'-dithiopropionimidate dihydrochloride (DTBP; Sigma-Aldrich, catalogue no. D2388) in DMEM-HEPES solution for 5 min at 37°C . DTBP was removed and quenched with 200 mM Tris-HCl (pH 8) (Sigma-Aldrich, catalogue no. 252859) for 2 min at room temperature. Cells were washed twice with ice-cold PBS and lysed in modified radioimmunoprecipitation assay buffer (RIPA, 50 mM Tris-HCl (pH 7.6), 150 mM NaCl, 5 mM disodium EDTA (pH 8), 0.5% w/v SDS, 1% v/v Triton X-100 and 1% v/v sodium deoxycholate in ddH₂O) for 2 min at 37°C .

Cell bodies were removed using a high-pressure water wash. Protein complexes remaining attached to dishes were washed in cold PBS and recovered in 100 µl of adhesion complex recovery solution (125 mM Tris-HCl (pH 6.8), 1% w/v SDS and 150 mM dithiothreitol (DTT)) by scraping. Protein complexes were then precipitated overnight using four volumes of -20°C acetone at -80°C . Precipitated proteins were centrifuged at 16,000 g for 20 min at 4°C and protein pellets washed with -20°C acetone (16,000 g , 20 min, 4°C). Proteins were then allowed to dry at room temperature for about 20 min. Precipitated complexes were resuspended in 2x reducing sample buffer (RSB, 50 mM Tris-HCl (pH 6.8), 10% (v/v) glycerol, 4% (w/v) SDS, 0.004% (w/v) bromophenol blue and 15% (v/v) β -mercaptoethanol) and heated to 70°C for 10 min and then heated for 3 min at 95°C .

In-gel tryptic digest of adhesion complexes and LC-MS/MS. Protein samples were loaded on 4–15% polyacrylamide gels and electrophoretically separated for 3 min at 200 V to allow proteins to fully migrate into the gel. Gels were then stained with Coomassie Blue solution (Bio-Rad) for 10 min at room temperature, and protein-bands were cut into 1 mm³ pieces and transferred to a 96-well PVDF plate (FiltrEx, Corning, catalogue no. 3504) with a pore size of 0.2 µm. Gel pieces were then washed with a freshly prepared 25 mM NH_4HCO_3 (Sigma-Aldrich) solution in H₂O followed by another wash in 100% (v/v) acetonitrile to dry the pieces. Samples were then washed twice with 100% (v/v) acetonitrile for 5 min and gel pieces dried using a vacuum centrifuge for 30 min at room temperature. Proteins were reduced by incubation in 10 mM DTT diluted in 25 mM NH_4HCO_3 for 1 h at 56°C and alkylated in 55 mM iodoacetamide diluted in 25 mM NH_4HCO_3 for 45 min at room temperature in the dark. Samples were washed using alternating 25 mM NH_4HCO_3 and acetonitrile for 5 min each and gels dried for 25 min at room temperature in the vacuum centrifuge. A 50 µl aliquot of 12 µg trypsin (Pierce) in 25 mM NH_4HCO_3 was added to each sample and incubated for 15 min at 4°C followed by an overnight incubation at 37°C . Upon digestion, peptides were extracted using 100% (v/v) acetonitrile in 0.2% (v/v) formic acid (FA, Thermo Fisher Scientific) for 30 min at room temperature followed by 50% (v/v) acetonitrile in 0.1% (v/v) FA into a clean tube. Peptides were dried using a vacuum centrifuge and subsequently resuspended in 5% (v/v) acetonitrile in 0.1% (v/v) FA to conduct desalting using 5 mg of POROS R3 beads (Applied Biosystems). Beads were conditioned using 50% (v/v) acetonitrile followed by adding 0.1% (v/v) FA in HPLC-grade water. Peptides were then washed using 0.1% (v/v) FA in HPLC-grade water and eluted in 30% (v/v) acetonitrile in 0.1% (v/v) FA, dried and resuspended in 5% (v/v) acetonitrile in 0.1% (v/v) FA for LC-MS/MS.

Peptides were analysed using an Ultimate 3000 RSLCnano system (Thermo Fisher Scientific) coupled to an Orbitrap Elite mass spectrometer (Thermo Fisher Scientific). Peptides were loaded onto a pre-column (200 mm \times 180 µm internal diameter, Waters) and separated on a bridged ethyl hybrid (BEH) C18 column (250 mm \times 75 mm internal diameter, 1.7 µm particle size, Waters) over a 2 h gradient from 8 to 33% (v/v) acetonitrile in 0.1% (v/v) FA at a flow rate of 200 nl min⁻¹. LC-MS/MS analysis was performed using a data-dependent mode to allow selection of peptide fragmentation in an automated manner. The resulting data were searched against the SwissProt database with species set to *Mus musculus* on an in-house Mascot server (Matrix Science; 2016) in Proteome Discoverer (Thermo Fisher Scientific, v.2.1). Search parameters included peptide modifications for carbamidomethylation (C) as static modification and oxidation (M, P and K) as well as deamination (N, Q) as dynamic modification. A decoy database search was performed to determine the peptide false discovery rate (FDR) with the Percolator module. A 1% peptide FDR threshold was applied, peptides were filtered for high peptide confidence and minimum peptide length of six and finally, peptides without protein reference were removed. All proteins that exhibited a confidence of less than 'high' and with less than two uniquely identified peptides were excluded from further analysis.

ECM enrichment of murine pancreatic tumours. ECM enrichment was conducted as described previously²⁰. In brief, tumours were snap-frozen in liquid nitrogen upon excision from diseased animals, histologically verified as PDA and stored at -80°C until preparation. For normal pancreata, the organs were excised from ten healthy C57-BL/6 animals and immediately flash-frozen in liquid nitrogen. Care was taken to remove excess fat from the pancreas prior to preparation. Frozen samples were then weighed, minced using a mortar and pestle in the presence of liquid nitrogen and resuspended in lysis buffer (buffer C (Merck Millipore) supplemented with 1x protease inhibitor (Merck Millipore)) to a final concentration of 10 mg per 100 µl lysis buffer. ECM proteins were enriched from 50 mg of the sample (500 µl buffer homogenate) material using the Compartment Protein Extraction Kit (Merck Millipore) according to the manufacturer's instructions. In brief, cytosolic, nuclear, membranous and cytoskeletal proteins were extracted, and ECM proteins were washed twice in buffer W and three times in PBS before sample preparation for mass spectrometry. All buffers were supplemented with 1x protease inhibitor (Merck Millipore), and buffer N was supplemented with 3.5 µl Benzoinase (Thermo Fisher Scientific) to digest genomic DNA and RNA. Extractions were conducted at least three times on separate days for all tumour samples unless otherwise stated. For the derivation of a normal pancreas matrixome atlas and to verify the consistency of the method, ten pancreata were combined, minced and obtained as homogenate. Ten individual

extractions were performed in batches of five on two consecutive days to control for intra- and inter-extraction variability.

S-Trap-based tryptic digestion of ECM-enriched fractions and LC-MS/MS.

ECM proteins were prepared for LC-MS/MS using S-Trap Midi Columns (Protifi). Samples were pulverized with frozen urea and resuspended in 8 M urea supplemented with 5% w/w SDS, 20 mM HEPES and 50 mM triethylammonium bicarbonate (TEAB) and harshly sonicated. Samples were then reduced in 5 mM tris(2-carboxyethyl)phosphine (Sigma-Aldrich) for 2 h at 37 °C and 1,400 r.p.m. (Thermomixer) and alkylated using 15 mM S-methyl methanethiosulfonate (MMTS, Sigma-Aldrich) for 30 min at room temperature. Urea was then diluted to 2 M by adding 50 mM TEAB and proteins were deglycosylated using PNGaseF (New England Biolabs) for 2 h at 37 °C and 1,400 r.p.m. Following sonication, samples were acidified to a final concentration of 1.2% (v/v) phosphoric acid (Fisher) and dissolved in S-Trap binding buffer (STBB, 90% v/v aqueous methanol and 0.1 M TEAB (pH 7.1)) at a volumetric ratio of 1:7 lysate:STBB. The acidified SDS-containing lysate in STBB was then spun into the S-Trap Midi Spin Columns (Protifi) at 4,000 g for 30 s to trap the proteins until the entire protein-containing lysate was passed through the columns. Trapped proteins were then washed with STBB four times, and proteins were digested overnight at 37 °C in 50 mM TEAB using sequencing-grade trypsin at a ratio of 1:10 in a humidified incubator. Following digestion, peptides were eluted in 500 µl 50 mM TEAB followed by 500 µl 0.2% FA in LC-grade water and 500 µl 50% acetonitrile supplemented with 0.2% FA in LC-grade water at 4,000 g for 60 s each. Peptides were then dried down and desalted using Sep-Pak Vac 3cc tC18-cartridges (Waters, catalogue no. WAT036820) according to the manufacturer's instructions. In brief, following equilibration of the C18 cartridges with 100% acetonitrile supplemented with 0.1% FA and 0.05% TFA in LC-grade water, samples were loaded in 0.05% TFA in LC-grade water and washed with 0.05% TFA in LC-grade water followed by washing with 0.1% FA in LC-grade water. Peptides were then eluted in 30% acetonitrile in LC-grade water and, following drying in a speedvac at 60 °C for 2 h, peptides were resuspended in 0.05% v/v TFA for LC-MS/MS. Next, 5.55 ng worth of peptide in 10 µl of 0.05% TFA were trapped on a PepMap 300 (C18, 300 µm × 5 mm, Thermo Fisher Scientific) column and separated on an EASY-Spray RSLC C18 columns (75 µm × 500 mm, Thermo Fisher Scientific, catalogue no. ES803) at 220 µl min⁻¹ using the following gradient profile (minutes:%B): 0:3.0, 45:33, 46:45, 47:80, 49:80, 50:3.0, 70:3.0. Buffer A consisted of 0.1% FA in LC-grade water and buffer B of 100% acetonitrile. The eluent was directed into an EASY-Spray source (Thermo Fisher Scientific) with temperature set to 60 °C and a source voltage of 1.9 kV. Data were acquired on QExactive HFX (Thermo Fisher Scientific) with precursor scan ranging from 375 to 1,200 m/z at 120,000 resolution and automatic gain control target of 3 × 10⁶. The isolation window was set to 1.5 m/z. dd-MS² scans were conducted at 30,000 resolution and automatic gain control target of 1 × 10⁵ and normalized collision energy set to 29%. At least four injections of each sample were conducted for each analysed tumour. For normal pancreas samples, at least five injections were conducted.

The resulting data were analysed in Progenesis (v.26.45.1656 Nonlinear Dynamics) using a Hi3 approach for each individual replicate and searched against the SwissProt database with species set to *M. musculus* on an in-house Mascot server (Matrix Science, 2016) using Mascot Daemon (v.2.6, Matrix Science). Search parameters included peptide modifications for methylthio (C) as static modifications and oxidation (M) as well as deamination (N, Q) as dynamic modifications. Only 2⁺, 3⁺ and 4⁺ charged peptide ions with a peptide tolerance of 10 ppm were included in the search. A 1% peptide FDR threshold was applied, peptides were filtered for high peptide confidence and a minimum peptide length of six and finally, peptides without protein reference were removed.

S-Trap-based tryptic digestion of whole cell lysates from synthetic hydrogels.

For LC-MS/MS analysis of cell-laden hydrogels, organoids were grown in PEG CBF-0.5 gels for 4 days from single-cell suspension in full organoid growth media as previously described. At the endpoint, gel plugs were removed from the 24-well plates, washed twice with PBS for 5 min each and, following removal of PBS, gel plugs were minced using a mortar and pestle with liquid nitrogen. The resulting fine powder was allowed to thaw to room temperature, resuspended in a solution of 4% v/v SDS, 50 mM TEAB and 20 mM HEPES (pH 7.8) and sonicated, and then 1 µl RNase was added per 100 µl lysate and the dissociation of genomic DNA and RNA was allowed to proceed for 30 min at room temperature. The lysate was then vigorously vortexed and clarified by centrifuging for 20 min at 16,000 g at room temperature. Following quantification of protein content using the BCA kit (Thermo Fisher Scientific) according to the manufacturer's instructions, an 80 µg aliquot of the lysate was subjected to S-Trap-based digestion using S-Trap Micro Spin Columns (Protifi). Briefly, proteins were reduced by adding 20 mM DTT (Sigma-Aldrich) for 10 min at 95 °C followed by alkylation with 40 mM IAA (Sigma-Aldrich) for 30 min in the dark at room temperature. Undissolved matter was then spun out and samples were acidified using 12% v/v phosphoric acid, which was added to a final concentration of 1.2% v/v. Next, the SDS-containing lysate was mixed with S-Trap binding buffer (90% v/v methanol and 0.1 M TEAB (pH 7.1)) at a volumetric ratio of 1:7 lysate:STBB. The acidified SDS-containing lysate in STBB was then spun into the S-Trap Micro Spin Columns (Protifi) at

4,000 g for 30 s to trap the proteins until the entire protein-containing lysate had passed through the columns. Trapped proteins were then washed with STBB four times and proteins were digested overnight at 37 °C in 50 mM TEAB using 4 µg of sequencing-grade trypsin (mass ratio 1:20 protein:trypsin). Following digestion, peptides were eluted in 50 mM TEAB, then 0.2% FA in LC-grade water and finally, in 50% acetonitrile and 0.2% FA in LC-grade water. Eluents were combined and peptides were dried down and stored at -80 °C until fractionation.

High-pH offline fractionation and LC-MS/MS. Peptides were fractionated as previously described²⁶. Briefly, peptides were separated on a Zorbax Extend-C18 column (4.6 mm × 150 mm, 3.5 µm, Agilent Technologies) at 250 µl min⁻¹ using the following gradient profile (minutes:%B): 5:0.5, 20:30, 24:40, 26:75, 29:75, 30:0.5, 55:0.5. Buffer A consisted of LC-grade water supplemented with 0.1% v/v NH₄OH (pH 10.5), and buffer B of 100% acetonitrile. The eluent was directed onto 96 round-bottom plates and fractions were collected every 15 s. Only fractions in the elution window between 15:50 and 35:00 min were used, and all of the fractions were concatenated into 24 final fractions, with each containing 3.33 µg peptide on average. Following drying in a speedvac at 60 °C for 2 h, peptides were resuspended at 100 ng ml⁻¹ in 0.05% v/v TFA for LC-MS/MS. Next, 100 ng of peptides were trapped on a PepMap 300 (C18, 300 µm × 5 mm, Thermo Fisher Scientific) column and separated on an EASY-Spray RSLC C18 column (75 µm × 500 mm, Thermo Fisher Scientific, catalogue no. ES803) at 200 nl min⁻¹ using the following gradient profile (minutes:%B): 6:1.0, 40:24, 45:45, 46:80, 49:80, 50:1.0, 70:1.0. Buffer A consisted of 0.1% FA in LC-grade water and buffer B of 100% acetonitrile. The eluent was directed into an EASY-Spray source (Thermo Fisher Scientific) with temperature set at 60 °C and a source voltage of 1.9 kV. Data were acquired on QExactive HFX (Thermo Fisher Scientific) with precursor scan ranging from 375 to 1,200 m/z at 120,000 resolution and automatic gain control target of 3 × 10⁶. The isolation window was set to 1.5 m/z. dd-MS² scans were conducted at 30,000 resolution and automatic gain control target of 1 × 10⁵ and normalized collision energy set to 29%.

The resulting data were searched against the SwissProt database with species set to *M. musculus* on an in-house Mascot server (Matrix Science, 2016) in Proteome Discoverer (Thermo Fisher Scientific, v.2.1). Search parameters included peptide modifications for carbamidomethylation (C) as static modification and oxidation (M, P and K) as well as deamination (N, Q) as dynamic modification. A decoy database search was performed to determine the peptide FDR with the Percolator module. A 1% peptide FDR threshold was applied, peptides were filtered for high peptide confidence and a minimum peptide length of 6 and finally, peptides without protein reference were removed. Protein grouping was performed by applying strict parsimony principles. All proteins that exhibited a confidence lower than 'high' and with fewer than two uniquely identified peptides were excluded from further analysis.

Electron microscopy. Samples were extensively washed with PBS and fixed with 4% formaldehyde and 2.5% glutaraldehyde in 0.1 M HEPES buffer (pH 7.2). Subsequently, samples were postfixed with 1% osmium tetroxide and 1.5% potassium ferricyanide in 0.1 M cacodylate buffer (pH 7.2) for 1 h, then 1% tannic acid in 0.1 M cacodylate buffer (pH 7.2) for 1 h and finally, in 1% uranyl acetate in water for 1 h. The samples were then dehydrated in ethanol, series-infiltrated with TAAB 812 resin and polymerized for 24 h at 60 °C. Sections were cut with a Reichert Ultracut ultramicrotome and observed with an FEI Tecnai 12 Biotwin microscope at 100 kV accelerating voltage. Images were taken with a Gatan Orius SC1000 CCD camera.

Live imaging of pancreatic cancer organoid co-cultures. CBF-0.5 hydrogels containing mPCOs, PaFs and BMDMs at a 1:5:5 ratio of PDO:PaF:BMDM were prepared as described previously and crafted into 10 µl domes in 24-well Sensoplates (Greiner). Co-culture domes were imaged via the PerkinElmer Opera Phenix microscope. A Zeiss EC Plan Neofluar ×10 air objective (NA 0.3, WD 5.2 mm) or Zeiss W Plan-Apochromat ×20 water objective (NA 1.0, WD 1.17 mm) were used as indicated. Pre-scan directed z-stack acquisition of individual spheres within the gel was used, and co-cultures were imaged every hour over a time window of 72 h starting from day 3 of culture. Videos and representative still images were generated from maximum intensity projections using Harmony 4.8 software. Representative images were exported from Harmony 4.8 in the portable network graphic format with scaling equally applied to all conditions.

ELISA. Concentrations of GM-CSF (catalogue no. DY415-05), IL6 (catalogue no. DY406-05), IL1α (catalogue no. DY400-05), IL1β (catalogue no. DY401-05), TNFα (catalogue no. DY410-05), CXCL12 (catalogue no. DY453-05) and TGFβ (catalogue no. DY1679-05) (all from R&D Systems) in organoid cultures were measured using ELISA DuoSet kits as per the manufacturer's instructions. In brief, CBF-0.5 hydrogels were dissociated using Sortase A pentamutant (SrtA), PBS was removed and 200 µl of 1 mg ml⁻¹ SrtA was added to the gels for 30 min at 37 °C before addition of 18 mM Gly-Gly-Gly (GGG) and 10 mM CaCl₂ and a further incubation of 20 min at 37 °C. Following dissociation, samples were supplemented with EDTA-free Protease Inhibitor Cocktail Set III and frozen at -80 °C. Samples were thawed and centrifuged at 14,000 g for 30 min at 4 °C. Supernatants were

mixed in a 1:1 (v/v) ratio with conditioned medium collected from the respective condition and were used for ELISA assay.

Cell viability analysis. PaFs were encapsulated in either synthetic hydrogel or Matrigel in combination with mPCOs and/or BMDMs as previously described and cultured for 6 days in hPOCM supplemented with 50 ng ml⁻¹ EGF and 20 ng ml⁻¹ M-CSF or reduced media (minimal media) as indicated. Single-cell suspensions were prepared using 0.25% v/v Trypsin-Versene Solution. Following neutralization with DMEM 10% v/v FBS and centrifugation, cells were resuspended at 1 × 10⁶ cells ml⁻¹ in PBS. Cells were incubated with LIVE/DEA Fixable Blue Dead Cell Stain (1/1,000, Thermo Fisher Scientific) at room temperature for 30 mins. Following washing in PBS, cells were resuspended in Cell Staining Buffer (CSM; Fluidigm) containing 5 mM EDTA, hereafter named CSM-1, supplemented with Fc block and subjected to surface staining with phycoerythrin-conjugated anti-CD45 (1:200, BioLegend, clone 30-F11) for 45 min on ice. Following staining, cells were washed in PBS, passed through a 70 µm filter and resuspended at a concentration of 1 × 10⁶ cells ml⁻¹ and analysed on an LSRFortessa X-20 flow cytometer (BD) using 355 nm, 488 nm, 561 nm and 640 nm lasers, with 450/50, 515/20, 586/15 and 730/45 filter sets, respectively. Cell-line-specific events were selected based on GFP positivity (PaF), iRFP positivity (mPCO) and CD45 positivity (BMDM), and viable cells were selected based on negativity for LIVE/DEAD blue stain.

Sample preparation for mass cytometry. To identify cells in synthesis phase (S phase), 5-iodo-2'-deoxyuridine (Sigma-Aldrich) was added to organoid culture medium at a final concentration of 25 µM and incubated for 30 min at 37 °C. Gels were then either dissociated immediately or fixed in 4% PFA for 60 min at 37 °C, washed twice in PBS (Fisher) and stored at 4 °C until needed. Both fixed and unfixed PEG-VS hydrogels were dissolved using SrtA (Supplementary Methods). The resultant solution was transferred to a gentleMACS C-Tube (Miltenyi) containing 0.5 mg ml⁻¹ Dispase II (Sigma), 0.2 mg ml⁻¹ Collagenase IV (Gibco) and 0.2 mg ml⁻¹ DNase (Gibco), made up to 5 ml in PBS and processed using the gentleMACS Octo Dissociator (with heaters; Miltenyi) at 37 °C for 50 min using a custom program adapted from Qin et al.⁵⁹. C-tube was spun at 1,000g for 1 min to collect all cellular material in the bottom of the tube. Cells were washed in 5 ml of PBS and passed through a 70 µm filter (BD) into polypropylene FACS tubes (BD Falcon) to remove residual cell clusters.

Mass cytometry analysis of PEG-VS hydrogel co-cultures. Methanol permeabilization. Fixed single-cell suspensions were washed in CSM-1. Cells were then pelleted by centrifugation; this and all subsequent centrifugations were performed at 1,000g for 5 min. Supernatant was removed and cells were vortexed in the void volume before addition of 2 ml of ice-cold 20% methanol for 20 min at -20 °C. Following incubation, cells were washed twice in 3 ml CSM-1 and the cell pellet was resuspended in the void volume. Next, 1 µl of Fc block was added for 5 min at room temperature, after which 50 µl of the heavy-metal tagged antibody master mix was added to 50 µl CSM and incubated for 45 min at room temperature (Supplementary Table 2). Following antibody incubation, cells were washed twice with CSM-1. The resultant pellet was resuspended in 200 µl PBS, 4% PFA was added under vortex and it was stored overnight at 4 °C.

FOXP3 Fix/Permeabilization. Unfixed single-cell suspensions were washed in CSM-1. Cells were then pelleted by centrifugation at 500g for 5 min. Supernatant was removed and cells were vortexed in the void volume before the addition of 1 µl Fc block (BD Biosciences) for 5 min at room temperature. Extracellular heavy-metal tagged antibody master mix (Supplementary Table 2) was added to 50 µl CSM and incubated for 45 min at room temperature. Following incubation, cells were washed twice with CSM-1. FOXP3 Fix/Perm Staining Buffer set (Invitrogen) was then used to fix and permeabilize the cells according to the manufacturer's instructions. In brief, cell pellets were resuspended in 1x Thermo FOXP3 Fix Buffer and incubated for 30 min at room temperature. Next, 2 ml of 1x Thermo FOXP3 perm buffer was added and cells pelleted. A further 2 ml of 1x Thermo FOXP3 perm buffer was added and cells pelleted. The cell pellet was resuspended in the void volume and 1 µl of Fc block added for 5 min at room temperature. Next, 50 µl of the intracellular heavy-metal tagged antibody master mix was added in 50 µl CSM and incubated for 45 min at room temperature. Following antibody incubation, cells were washed twice with CSM-1. The resultant pellet was resuspended in 200 µl PBS, 4% PFA was added under vortex and it was stored overnight at 4 °C.

All samples were processed similarly from this point. The following day, 1 µl of iridium solution (Fluidigm) was added per 3 × 10⁶ cells followed by incubation for 60 min at room temperature. The cell suspension was diluted 1:3 in PBS before pelleting. Cells were washed in Maxpar water (Fluidigm) and resuspended in Maxpar water containing 15% (v/v) EQ beads (Fluidigm) to a concentration of 10⁶ cells per ml and filtered twice (70 µm) before measuring on a Helios mass cytometer (Fluidigm) (300–500 events per second). Files were normalized against EQ beads, de-barcode and uploaded to the CytoBank platform (<http://www.cytobank.org/>). Cell doublets and aggregates were removed based on event length. Live cell events were selected based on cleaved caspase-3 negativity. Cell-line-specific events were selected based on GFP positivity (PaF) and CD45

positivity (BMDM). Selected populations were exported as FCS files and uploaded to the Cytofit2 package (v.2.0.1). Cells were clustered using FlowSOM and visualized using UMAP projections and expression overlays, and cell data with annotated clusters were exported for further downstream analysis of marker expression using R Studio v.4.0.0 (<https://www.r-project.org/>).

Survival analysis. For comparison of matrisomal protein changes between studies, supplementary data files from Tian et al.²⁵ were downloaded, and Log2FC between PDA and NP samples were used from either the murine or human cohort. For the human cohort, all samples were used regardless of differentiation grade. Using R v.4.0.0, we computed the Pearson or Spearman-based rank correlation of the Log2FC(PDA/WT) of matrisomal proteins identified and quantified in this study and Tian et al.²⁵. For survival analysis, matrisomal proteins with a Log2FC(PDA/WT) ≥ 1 in this study and Tian et al.²⁵ were used, and gene identifiers were translated into `entrezgene_ids` using the `biomaRt` R package⁶⁰. Clinical information and gene-expression data for human pancreatic cancer (TCGA-PAAD) were downloaded from cBioPortal (accessed 22 April 2020; refs. ^{61,62}) and `log2` transformed. The Cox-proportional hazard regression *P* value and hazard ratio were determined in quantile-categorized patients (top 25% versus bottom 25%) by the matrisomal protein expression for the TCGA dataset (*n* = 179). The survival analysis was done using the survival package (v.3.2–3, <https://cran.r-project.org/web/packages/survival/index.html>) and Kaplan–Meier survival plots were computed using the `survminer` R package in R v.4.0.0.

Bioinformatics and statistics. Bioinformatics were conducted using the open-source R software (v.4.0.0). Proteins with matrisomal origin were annotated from proteomic datasets using the murine matrisome⁶³. Proteins with BM origin were annotated from matrisome using the gene ontology term 'basement membrane' (GO:0005604; <http://www.informatics.jax.org/go/term/GO:0005604>, accessed 5 October 2020 (ref. ⁶⁴)). Pathway annotations based on the Kyoto Encyclopaedia of Genes and Genomes (KEGG), gene ontology term annotations and biological process term annotations were obtained from the database for annotation, visualization and integrated discovery (DAVID) functional annotation clustering by assuming the whole genome as statistical background. For gene ontology and biological process term enrichment, only terms with at least three members, an FDR ≤ 0.05, Benjamini–Hochberg adjusted *P* value ≤ 0.05 and fold enrichment of ≥ 1.5 were included. For KEGG-pathway annotation, only pathways with at least three members, a *P* value ≤ 0.05 and fold enrichment ≥ 1.5 were included. MatriCircos plots were generated using the open-source RCircos R package⁶⁵ by applying a custom-made RCircos core-component library containing previously annotated core-matrisome proteins only. Circular visualizations of YAP1 nuclear/cytoplasmic ratio were implemented using the `circize` R package⁶⁶. Integrin–ECM interactions were obtained from a publicly available manually curated cell–cell interaction database from the Bader lab (<https://baderlab.org/CellCellInteractions>), and only literature-based interactions with PubMed annotation were included in the analysis. For integrin–ECM interactions, only those interactions nucleating from an integrin α subunit were considered and integrin complexes containing an α and β subunit were subsequently manually assembled. For network analysis and protein–interaction network visualization, the cytoscape software package⁶⁷ was used by incorporating the String database (STRING CONSORTIUM, v.10.5, 2018 (ref. ⁶⁸)), MCODE and boundaryLayout apps). For String-based network visualization, networks were curated using a very stringent confidence of 0.95 by accepting text-mining, experimental, database, co-expression, neighbourhood, gene-fusion and co-occurrence interaction sources to obtain relevant integrin–ECM interactions. Statistics and visualizations were conducted using GraphPad Prism v.8 or R v.4.0.0. For statistical analysis of high-content imaging data, the non-parametric two-tailed Wilcoxon *t*-test was utilized with application of Benjamini–Hochberg correction and an FDR threshold of 0.05 in R. For statistical analysis of adhesion assays and PDO growth assessments in stiffened hydrogels, the parametric two-tailed Student's *t*-test was conducted with application of Benjamini–Hochberg correction and an FDR threshold of 0.05 in R. For statistical analysis of lebein-2 treated organoids, the two-tailed parametric paired Student's *t*-test was used. For statistical analysis of YAP1 ratio between stiffened hydrogels, the parametric two-sided Student's *t*-test was used to compare 1.4, 3.1 and 8.2 kPa conditions whilst the non-parametric Wilcoxon test was utilized for comparison of 1.4 and 20.5 kPa conditions upon removal of outliers and with application of Benjamini–Hochberg correction and an FDR threshold of 0.05 in R. Outliers were identified and removed from each population when exceeding 1.5 times the interquartile range and confirmed as outliers by the Grubb's test function from the outliers package in R v.4.0.0. Normality was assessed in R using the Shapiro–Wilk test with a significance level of 0.05.

Reporting Summary. Further information on research design is available in the Nature Research Reporting Summary linked to this article.

Data availability

All original source data are freely available. The mass spectrometry proteomics data have been deposited to the ProteomeXchange Consortium via the PRIDE⁶⁹ partner

repository with the following dataset identifiers: NP matrisome atlas (PXD022555 and 10.6019/PXD022555); IAC datasets (PXD022487 and 10.6019/PXD022487); cell-derived matrix datasets (PXD022509 and 10.6019/PXD022509); 3D PEG CBF-0.5 LC-MS (PXD022520 and 10.6019/PXD022520); Tumour Matrisome LC-MS (PXD022767 and 10.6019/PXD022767). Raw CyTOF data, IF images and AFM force curves as well as source data for all figures (Figs. 1–5 and Supplementary Figs. 1–28) have been deposited to <https://zenodo.org/record/4664132>.

Code availability

All original R scripts have been deposited to <https://zenodo.org/record/4664132> and are freely available.

References

- Wu, J. et al. Generation of a pancreatic cancer model using a *Pdx1-Flp* recombinase knock-in allele. *PLoS ONE* **12**, e0184984 (2017).
- Ouyang, H. et al. Immortal human pancreatic duct epithelial cell lines with near normal genotype and phenotype. *Am. J. Pathol.* **157**, 1623–1631 (2010).
- Furukawa, T. et al. Long-term culture and immortalization of epithelial cells from normal adult human pancreatic ducts transfected by the *E6E7* gene of human papilloma virus 16. *Am. J. Pathol.* **148**, 1763–1770 (1996).
- Huch, M. et al. Unlimited in vitro expansion of adult bi-potent pancreas progenitors through the Lgr5/R-spondin axis. *EMBO J.* **32**, 2708–2721 (2013).
- Bankhead, P. et al. QuPath: open source software for digital pathology image analysis. *Sci. Rep.* **7**, 16878 (2017).
- Schindelin, J. et al. Fiji: an open-source platform for biological-image analysis. *Nat. Methods* **9**, 676–682 (2012).
- Livak, K. J. & Schmittgen, T. D. Analysis of relative gene expression data using real-time quantitative PCR and the $2^{-\Delta\Delta C_t}$ method. *Methods* **25**, 402–408 (2001).
- Qin, X. et al. Cell-type-specific signaling networks in heterocellular organoids. *Nat. Methods* **17**, 335–342 (2020).
- Durinck, S., Spellman, P. T., Birney, E. & Huber, W. Mapping identifiers for the integration of genomic datasets with the R/Bioconductor package biomaRt. *Nat. Protoc.* **4**, 1184–1191 (2009).
- Cerami, E. et al. The cBio cancer genomics portal: an open platform for exploring multidimensional cancer genomics data. *Cancer Discov.* **2**, 401–404 (2012).
- Gao, J. et al. Integrative analysis of complex cancer genomics and clinical profiles using the cBioPortal. *Sci. Signal* **6**, pl1 (2013).
- Naba, A. et al. The extracellular matrix: tools and insights for the ‘omics’ era. *Matrix Biol.* **49**, 10–24 (2016).
- Bult, C. J. et al. Mouse genome database (MGD) 2019. *Nucleic Acids Res.* **47**, D801–D806 (2019).
- Zhang, H., Meltzer, P. & Davis, S. RCircos: an R package for Circos 2D track plots. *BMC Bioinformatics* **14**, 244–245 (2013).
- Gu, Z., Gu, L., Eils, R., Schlesner, M. & Brors, B. Circlize implements and enhances circular visualization in R. *Bioinformatics* **30**, 2811–2812 (2014).
- Shannon, P. et al. Cytoscape: a software environment for integrated models of biomolecular interaction networks. *Genome Res.* **13**, 2498–2504 (2003).
- Szklarczyk, D. et al. The STRING database in 2017: quality-controlled protein–protein association networks, made broadly accessible. *Nucleic Acids Res.* **45**, D362–D368 (2017).
- Pérez-Riverol, Y. et al. The PRIDE database and related tools and resources in 2019: improving support for quantification data. *Nucleic Acids Res.* **47**, D442–D450 (2018).

Acknowledgements

This work was supported by Cancer Research UK Program grant no. C13329/A21671 (M.J.H., C.J.), Cancer Research UK Institute Awards A19258 (C.J.) and A17196 (J.P.M.), Experimental Medicine Programme Award A25236 (C.J. and J.P.M.), Rosetrees Trust grant no. M286 (C.J.), European Research Council Consolidator Award ERC-2017-COG 772577 (C.J.), National Science Foundation grant no. CBET-0939511 (L.G.G.), National Institutes of Health grants no. R01EB021908 and T32GM008334 (L.G.G.) and Defense Advanced Research Projects Agency grant no. W911NF-12-2-0039 (L.G.G.). J.A.E. is financially supported by the Deutsche Forschungsgemeinschaft (DFG grant no. SFB1009 project A09). We thank D. Liu, A. Thrasher, T. Roberts, B. Torok-Storb, I. Verma, D. Trono and T. Somerville for kindly sharing plasmids, M.-S. Tsao (UHN) for HPDE H6c7 cells, M. Ball and E. Mckenzie at Manchester Institute of Biotechnology for sortase expression and purification, C. J. Tape at University College London for technical advice, K. Beattie for assistance at FingerPrints Proteomics Facility (University of Dundee), the Cancer Research UK Glasgow Centre (A25142), the Biological Service Unit facilities at CRUK BI and members of Systems Oncology Group at CRUK MI for constructive input.

Author contributions

C.R.B., J.K., A. Brown, B.Y.L., J.D.H., D.L.S., L.G.G., M.J.H. and C.J. designed the research; C.R.B., J.K., A. Brown, A. Banyard, J.D.H., J.X., C.L., D.K., A.M., N.H., D.L.S., J.B., C.C. and B.Y.L. conducted experiments; C.R.B., J.K., A. Brown, A. Banyard and C.J. analysed data; A. Banyard, C.C., V.H.-G., L.S., J.A.E., B.S., X.Z., D.L.S., D.K., J.A., G.A. and C.H. provided technical support; J.P.M. maintained the genetically engineered murine models and provided murine samples; J.P.M., L.S., L.G.G., J.A.E. and B.S. provided reagents and cell lines; M.A.G., J.G., L.F. and D.A.O. helped with clinical sample collection; L.F. provided pathological support; C.R.B. and C.J. wrote the paper and C.J. and L.G.G. oversaw the project. J.X. contributed to this work while an employee at CRUK MI.

Competing interests

L.G.G. has patent application pending related to the hydrogel system. The rest of the authors have no competing interests.

Additional information

Supplementary information The online version contains supplementary material available at <https://doi.org/10.1038/s41563-021-01085-1>.

Correspondence and requests for materials should be addressed to Linda G. Griffith or Claus Jørgensen.

Peer review information *Nature Materials* thanks the anonymous reviewers for their contribution to the peer review of this work.

Reprints and permissions information is available at www.nature.com/reprints.

Reporting Summary

Nature Research wishes to improve the reproducibility of the work that we publish. This form provides structure for consistency and transparency in reporting. For further information on Nature Research policies, see [Authors & Referees](#) and the [Editorial Policy Checklist](#).

Statistics

For all statistical analyses, confirm that the following items are present in the figure legend, table legend, main text, or Methods section.

n/a Confirmed

- The exact sample size (n) for each experimental group/condition, given as a discrete number and unit of measurement
- A statement on whether measurements were taken from distinct samples or whether the same sample was measured repeatedly
- The statistical test(s) used AND whether they are one- or two-sided
Only common tests should be described solely by name; describe more complex techniques in the Methods section.
- A description of all covariates tested
- A description of any assumptions or corrections, such as tests of normality and adjustment for multiple comparisons
- A full description of the statistical parameters including central tendency (e.g. means) or other basic estimates (e.g. regression coefficient) AND variation (e.g. standard deviation) or associated estimates of uncertainty (e.g. confidence intervals)
- For null hypothesis testing, the test statistic (e.g. F , t , r) with confidence intervals, effect sizes, degrees of freedom and P value noted
Give P values as exact values whenever suitable.
- For Bayesian analysis, information on the choice of priors and Markov chain Monte Carlo settings
- For hierarchical and complex designs, identification of the appropriate level for tests and full reporting of outcomes
- Estimates of effect sizes (e.g. Cohen's d , Pearson's r), indicating how they were calculated

Our web collection on [statistics for biologists](#) contains articles on many of the points above.

Software and code

Policy information about [availability of computer code](#)

Data collection

Orbitrap Elite mass spectrometer (Thermo) operated under Thermo XCalibur (V4.1.31.9) was used to acquire IAC LC-MS/MS data. OrbiTrap Velos Pro (Thermo) operated under Thermo XCalibur was used to acquire COM LC-M/MS data. QExactive HFX (Thermo) operated under Thermo XCalibur was used to acquire matrisome and PEG mPCO LC-MS/MS data. PerkinElmer Opera Phenix microscope and Harmony 4.8 (Perkin Elmer) software was used to acquire confocal images. Leica SP8 TCS inverted confocal microscope and LAS-X software suite (V3.5.5) (Leica) was used for second harmonic generation imaging. Li-COR Odyssey and Li-COR ImageStudio (V 5.2) was used for western blot imaging. Bruker Catalyst with a Nanoscope V controller (Bruker UK Ltd., Coventry UK) operating under nanoscope software (V9.1, Bruker) was used for AFM indentations. FEI Tecnai 12 Biotwin microscope operated under Tecnai User Interface software (V1.9) was used to acquire EM images. Helios mass cytometer (Fluidigm) operated under the CyTOF software (V7 Fluidigm) was used to acquire CyTOF data. Aria III SORP sorter (BD Biosciences) operated under BD Diva software (8.0) was used for FACS sorting. Leica SCN-400 operated under the Leica SCN-400 software suite (V 2.2.0.3789) was used to scan histology slides. Olympus VS-120 operated under the Olyvia software (V2.9, OLYMPUS) was used to scan IF slides. QuantStudio 5 Real-Time-PCR instrument (Applied Biosystems, Thermo) operated under the QuantStudio Design & Analysis software (V1.5.1, 2016, Applied Biosystems, Thermo) was used for RT-qPCR analysis.

Data analysis

Proteome Discoverer (V2.1, ThermoFisher) was used to analyze qualitative LC-MS/MS data (IAC, COM, 3D-PEG LC-MS/MS). Progenesis (V26.45.1656, Nonlinear Dynamics) was used to analyze qualitative LFC matrisome LC-MS/MS data (matrisome datasets). Harmony (V4.8, PerkinElmer) was used to analyze adhesion and high-content screening data and live imaging videos. Imaris (V9.5, Bitplane) was used for 3D analysis of co-culture images. ImageStudio Lite (V 5.2, Li-COR) was used to analyze western blot images. ImageScope (V12.3.3, Leica) was used to analyze histology slides. Olyvia (V2.9, OLYMPUS) has been used to acquire IF images. QuPath (V0.2.3) was used to analyze IF images and export high-quality IF images from scanned slides. QuantStudio Design & Analysis software (V1.5.1, 2016, Applied Biosystems, Thermo) was used to analyze and export RT-qPCR data.

CT-FIRE (V2.0, open source) was used to analyze SHG images.
 Fiji (V. 1.52e, NIH) was used to analyze microscopy images including IF and brightfield.
 NanoScope Analysis software (V4.8, Bruker) was used to analyze AFM data.
 Cytoscape (V3.8.2, National Resource of network biology) was used for network analysis using the plugins: MCODE (V2.0.0) , String app (V1.6.0), boundarylayout (V1.1).
 Cytobank.org and Cytofit2 package (version 2.0.1) were used to analyze Mass Cytometry data
 Prism GraphPad 8 (GraphPad Software Inc) was used for statistical analysis and data visualization.
 The R programming language (V4.0.0) using the packages (tidyverse V1.3.0, scales V1.1.1, rrcrize V0.4.13, biomaRt V2.44.0, RCircos V1.2.1, ggplot2 V3.3.0, ggpubr V0.3.0, ggsci V2.9, viridis V0.5.1, outliers V0.14, ggplot, Cytofit2 V2.0.1, flowSOM V1.4.0) was used to analyze raw data, conduct statistical testing and visualize data.

For manuscripts utilizing custom algorithms or software that are central to the research but not yet described in published literature, software must be made available to editors/reviewers. We strongly encourage code deposition in a community repository (e.g. GitHub). See the Nature Research [guidelines for submitting code & software](#) for further information.

Data

Policy information about [availability of data](#)

All manuscripts must include a [data availability statement](#). This statement should provide the following information, where applicable:

- Accession codes, unique identifiers, or web links for publicly available datasets
- A list of figures that have associated raw data
- A description of any restrictions on data availability

All original source data are freely available: The mass spectrometry proteomics data have been deposited to the ProteomeXchange Consortium via the PRIDE partner repository with the dataset identifiers: NP matrisome atlas (PXD022555 and 10.6019/PXD022555); IAC datasets (PXD022487 and 10.6019/PXD022487); CDM datasets (PXD022509 and 10.6019/PXD022509); 3D PEG CBF-0.5 LC-MS (PXD022520 and 10.6019/PXD022520); Tumour Matrisome LC-MS (PXD022767 and 10.6019/PXD022767). Raw CyTOF data, IF images and AFM force curves as well as source data for all figures (Figures 1-5 and Supplemental Figures 1-28) have been deposited to <https://www.zenodo.org/> (10.5281/zenodo.4664132). Clinical information and gene-expression data for human pancreatic cancer (TCGA-PAAD) were downloaded from cBioPortal (<https://www.cbioportal.org>, accessed: 22/04/2020)

Field-specific reporting

Please select the one below that is the best fit for your research. If you are not sure, read the appropriate sections before making your selection.

Life sciences Behavioural & social sciences Ecological, evolutionary & environmental sciences

For a reference copy of the document with all sections, see [nature.com/documents/nr-reporting-summary-flat.pdf](https://www.nature.com/documents/nr-reporting-summary-flat.pdf)

Life sciences study design

All studies must disclose on these points even when the disclosure is negative.

Sample size	No statistical measures were conducted to predetermine the sample size. All sample size, statistical tests and p-values are indicated in the figure legends and described in materials and methods under "Bioinformatics and Statistics". We chose the sample size to sufficiently determine significance in all experiments with focus on reproducible statistical analysis between the conditions. All analysis with human and murine organoids include replicates with independently isolated organoids. In general sample size was based on articles published on similar research topics (e.g. ref 16, 17, 19, 26,27, 36 and 38). For animal experiments, the 3R guidelines were closely followed to reduce the number of animals used in this study while retaining statistical power.
Data exclusions	No data was excluded from the study.
Replication	All experimental findings were verified in at least three independent biological replicates or in at least one orthogonal biological model system. All attempts at replication were successful.
Randomization	Samples were prepared, treated, processed and analysed in random order.
Blinding	Blinding was conducted during the pathological scoring on murine pancreatic cancer samples by a trained pathologist who was blinded to genotype, stage and/or data generated from any animal in this study. The remaining experiments were not blinded as the investigators who set up the experiments analysed the data, which is incompatible with blinding.

Reporting for specific materials, systems and methods

We require information from authors about some types of materials, experimental systems and methods used in many studies. Here, indicate whether each material, system or method listed is relevant to your study. If you are not sure if a list item applies to your research, read the appropriate section before selecting a response.

Materials & experimental systems

n/a	Involvement
<input type="checkbox"/>	<input checked="" type="checkbox"/> Antibodies
<input type="checkbox"/>	<input checked="" type="checkbox"/> Eukaryotic cell lines
<input checked="" type="checkbox"/>	<input type="checkbox"/> Palaeontology
<input type="checkbox"/>	<input checked="" type="checkbox"/> Animals and other organisms
<input type="checkbox"/>	<input checked="" type="checkbox"/> Human research participants
<input checked="" type="checkbox"/>	<input type="checkbox"/> Clinical data

Methods

n/a	Involvement
<input checked="" type="checkbox"/>	<input type="checkbox"/> ChIP-seq
<input type="checkbox"/>	<input checked="" type="checkbox"/> Flow cytometry
<input checked="" type="checkbox"/>	<input type="checkbox"/> MRI-based neuroimaging

Antibodies

Antibodies used

Antibodies used for Immunofluorescence/immunohistochemistry: OCT embedded samples (fresh frozen) for Immunofluorescence: -

- rabbit anti-ZO1 (1:100, Invitrogen, 61-7300)
- rat anti-CD49f (1:500, Merck Millipore, MAB1378, clone NKI-GoH3)
- rabbit anti-E-Cadherin (1:100, Cell Signalling, 3195, Clone 24E10)
- rabbit anti-Sox9 (1:300, Merck Millipore, AB5535)
- rabbit anti-Yap1 (1:50, Cell Signaling Technology, 4912s)
- rabbit anti-Laminin (1:50, abcam, ab11575)
- Alexa-488 conjugated donkey anti-Rabbit (1:400, Invitrogen, A21206)
- Alexa-488 conjugated donkey anti-Rat (1:400, Invitrogen, A21208)
- Alexa-647 conjugated goat anti-Rat (1:400, Invitrogen, A21247)

OCT embedded murine samples (fresh frozen) for immunohistochemistry:

- rabbit anti-F4/80 (1:100, Cell Signalling Technology, 70076)
- rabbit anti-PanCK (1:100, Abeam, ab9377)
- rat anti-CO45 (1:100, BO biosciences, 550539, clone 30-Fil)
- rabbit anti-Podoplanin (1:500, Thermo Fisher, MA5-29742)
- HRP conjugated goat anti-Rabbit secondary antibody (RTU, Oako, K4003)

OCT embedded human samples (fresh frozen) for immunohistochemistry:

- rabbit anti-Igga3 (1:1000, Merck Millipore, AB1920)
- rat anti-Igga6 (1:1000, Merck Millipore, MAB1378, Clone NKI-GoH3)
- rabbit anti-Igga2 (1:2000, Merck Millipore, AB1936)
- mouse anti-Itgav (1:3000 abeam, ab16821)
- rat anti-Itgb1 (1:3000, BO Biosciences, 550531, Clone 9EG7)
- mouse anti-Itgb4 (1:250, Merck Millipore, MAB2059, Clone ASC-8)
- mouse anti-Lamas (1:1000, Merck Millipore, MAB1924, Clone 4C7)
- mouse anti-PanCK (1:5000, Sigma Aldrich, C2931)

Formalin fixed murine samples for immunohistochemistry (in addition to antibodies previously mentioned):

- rabbit anti-F4/80 (1:100, Cell Signalling Technology, 70076)

Function-blocking antibodies:

- rabbit anti-Igga6 (10 ug/mL, Merck Millipore, MAB1378, Clone NKI-GoH3)
- mouse anti-Igga3 (10 ug/mL, ThermoFisher, 17-0494042, Clone PIBS)

Antibodies for Immunoblotting:

- mouse anti-Lamas (1:1000, Mybiosource MBS820658)
- rabbit anti-Gapdh (1:5000, abeam, ab181602)
- Dylight 800 (1:15,000, Cell Signalling Technologies) or 680 (1:15,000, Cell Signalling Technologies) 4xPEG pe-conjugated secondary antibodies

Antibodies used for Flow cytometry:

- brilliant violet 421 (BV-421) conjugated anti-CD45 (BioLegend Clone 30-Fil, #103133)
- BV-421 conjugated CD-31 (BioLegend, clone MEC13.3, #102423)
- BV-421 conjugated Anti-EpCAM (BioLegend clone G8.8, #118225)
- Phycoerythrin (PE) conjugated CD-90 (Thermo, clone G7, #A14726)
- PE-Cyanine7 (PE-Cy7) conjugated anti-podoplanin (PDPN, BioLegend, clone 8.1.1, #127411)

Antibodies used for Mass Cytometry:

- CD68 (BioLegend #137002, Clone FA-11)
- cC3 (CST, #9579, Clone 03E9)
- CD11b (eBioScience, 14-0112-81, Clone M1/70, # 14-0112-82)
- ITGA2 (BioLegend, 103501, Clone HMa2)
- Podoplanin (BioLegend, 127402, Clone 8.1.1)
- Pan Cytokeratin (BioLegend, 628602, Clone C11)
- Vimentin (CST, #5741, Clone 021H3)
- Desmin (abcam, ab216616, Clone Y66)

- aSMA (ThermoFisher, 14-9760-82, Clone A4)
- Ki67 (ThermoFisher, 14-5698-82, Clone: SoLA15)
- ITGA6 (Merck Millipore, MAB1378, Clone: NKI-GoH3)
- EpCam (Biolegend, 118202, Clone G8.8)
- CD206 (Biolegend, 141702, Clone Co68C2)
- ITGB1 (Biolegend, 102203, Clone HMBI-1)
- GFP (Biolegend, 338002, Clone FM264G)
- CD45 (BD Biosciences, 550994, Clone 30-F11)
- pRb (BD Biosciences, 558389, Clone J112-906)
- MHC Class 2 (eBioScience, 14-5321-81, Clone M5/114.15.2)

Validation

All antibodies used in this study have been verified either by the direct manufacturer or a competing manufacturer for the exact same clone for the application for which this antibody has been used in this study. Immunoblotting: Lama5 (Mybiosource MBS820658) species reactivity: mouse. (Yun et al., Cell Death Dis 2014 5(2):e1049). Gapdh (ab181602) species reactivity: mouse (Lu et al EMBO Mol Med 2021 13(1):e12798). IF and IHC: Zo1 (Invitrogen, 61-7300) species: mouse, human (Jorgens et al J Cell Sci 2017 1:177-189). CD49f (MAB1378, clone NKI-GoH3) species: mouse, human. E-Cadherin (Cell Signalling, 3195, Clone 24E10) species: mouse, human (Nikolopoulou et al Nat Commun 2019 10(1):2487). Sox9 (Merck Millipore, AB5535) species: mouse, human. Laminin (ab11575) species: human, mouse (Bisi et al., Nat. Commun. 2020 11(1):3516). F4/80 (Cell Signalling Technology, 70076) species: mouse (Lorscheid et al JCI Insight 2019 4(22):e130835). PanCK (ab9377) specie: human, mouse (Ligorio et al Cell 2019 178(1):160-175). CD45 (BD biosciences, 550539, clone 30-F11) species: mouse. Podoplanin (MA5-29742) species: mouse. Yap1 (Cell Signaling Technology, 4912s) species: mouse, the specificity of the antibody was validated against isotype control (Rabbit IgG Control antibody (Vector Laboratories, I-1000-5). Itga3 (AB1920) species: human. Itga6 (MAB1378, Clone NKI-GoH3) species: human. Itga2 (AB1936) species: human. Itgav (ab16821) species: human. Itgbl (Clone 9EG7) species: human. Itgb4 (MAB2059, Clone ASC-8) species: human. Lama5 (MAB1924, Clone 4C7) species human. PanCK (C2931) species human, mouse. For IF/IHC applications, the antibody signal has been compared against a non-primary antibody control and only those antibodies with a significantly higher signal/noise and background ratio as well as correct localization have been used in this study.

Function blocking: Itga6 (MAB1378, Clone NKI-GoH3) species: human, Itga3 (17-0494042, Clone PIBS) species: human. Samarelli, A. V. et al. Journal of Biological Chemistry, (2014) or Aumailley, M., Timpl, R. & Sonnenberg, Experimental Cell Research (1990).

For Mass Cytometry and flow cytometry applications, only antibodies reported by Fluidigm or manufacturers to be suitable for mass or flow cytometry respectively have been used in this study (Hutton et al Cancer Cell 2021 doi:10.1016.jccell.2021.060017 in press). CD68 (BioLegend #137002, Clone FA-11) species: mouse. cC3 (CST, #9579, Clone 03E9) species: mouse. CD11b (eBioScience, 14-0112-81, Clone MI/70, # 14-0112-82), species: mouse. ITGA2 (BioLegend, 103501, Clone HMa2), species: mouse. Podoplanin (BioLegend, 127402, Clone 8.1.1), species: mouse. Pan Cytokeratin (BioLegend, 628602, Clone C11), species: mouse. Vimentin (CST, #5741, Clone 021H3) species: mouse. Desmin (abcam, ab216616, Clone Y66) species: mouse. aSMA (ThermoFisher, 14-9760-82, Clone A4), species: mouse. Ki67 (ThermoFisher, 14-5698-82, Clone: SoLA15), species: mouse. ITGA6 (Merck Millipore, MAB1378, Clone: NKI-GoH3), species: mouse. EpCam (Biolegend, 118202, Clone G8.8), species: mouse. CD206 (Biolegend, 141702, Clone Co68C2), species: mouse. ITGB1 (Biolegend, 102203, Clone HMBI-1), species: mouse. GFP (Biolegend, 338002, Clone FM264G). CD45 (BD Biosciences, 550994, Clone 30-F11), species: mouse. pRb (BD Biosciences, 558389, Clone J112-906), species: mouse. MHC Class 2 (eBioScience, 14-5321-81, Clone M5/114.15.2), species: mouse.

Eukaryotic cell lines

Policy information about cell lines

Cell line source(s)

"Suit-2" - ATCC
 "iKras" - Ronald DePinho's lab at MD Anderson Cancer Research Centre
 "KPC-1" - Jennifer Morton's lab at CRUK Beatson Institute
 "KPC-43" - Kristopher Freese, CRUK Manchester Institute
 "HPDE" - Ming Tsao's lab at University Health Network (UHN), Toronto
 "HEK-FT" - Tim Somerville's lab at CRUK Manchester Institute.
 All other organoids and murine cell lines are isolated from genotyped animals (cancer organoids) or healthy animals (for PaFs and BMDMs).
 Human organoids were derived from resected specimens of pancreatic cancer patients with pathologically verified disease. Patient and clinical information for patient-derived samples are disclosed in Source data (<https://zenodo.org/record/4664132>).

Authentication

Organoids and murine cell lines are isolated from genotyped animals and genotype of organoid lines has been confirmed by ddPCR and Sanger sequencing. Human cell lines are regularly confirmed by STR profiling. Mutation status of Kras has been confirmed in human organoids using ddPCR.

Mycoplasma contamination

All cell lines and organoid lines in this manuscript are routinely tested for mycoplasma using qPCR and have been found negative.

Commonly misidentified lines (See [ICLAC](https://www.icscl.org/) register)

Commonly misidentified cell lines were not used in this study.

Animals and other organisms

Policy information about [studies involving animals](#); [ARRIVE guidelines](#) recommended for reporting animal research

Laboratory animals	KPC (KrasLSL-G12D/+; Trp53LSL-R172H/+; Pdx-1-Cre), KPF (KrasFrt-S-Frt-G12D/+; Trp53LSL-Frt; Pdx-1-Flp), KC (KrasLSL-G12D/+; Pdx-1-Cre) and KF (KrasFrt-S-Frt-G12D/+; Pdx-1-Flp) animals. Mice were maintained in purpose-built facility in a 12 hr light/dark cycle at uniform temperature and humidity with continual access to food and water. Age and gender of the laboratory animals are detailed in the source data (https://zenodo.org/record/4664132).
Wild animals	The study did not involve wild animals.
Field-collected samples	The study did not involve field collected samples.
Ethics oversight	All animal experiments were reported in accordance with the 'Animals (Scientific Procedures) Act of 1986' under project license No. 70/8745 (CRUK Manchester Institute) and 70/8375 (University of Glasgow). Conducted experiments with laboratory animals adhered to Animal Research: Reporting of In Vivo Experiments (ARRIVE) guidelines and were subjected to constant review by the Animal Welfare and Ethical Review Boards of the Cancer Research UK Manchester Institute and the University of Glasgow (UoG).

Note that full information on the approval of the study protocol must also be provided in the manuscript.

Human research participants

Policy information about [studies involving human research participants](#)

Population characteristics	For human patient-derived organoids and samples used for IHC/AFM, patient information and characteristics are disclosed in Supplementary Data 1. For expression analysis in human PDAC patients, data was obtained from the cancer genome atlas (TCGA) using cBioPortal (https://www.cbioportal.org/ , Cerami et al., 2012 & Gao et al., 2013). For population characteristics patient and clinical annotations for the PAAD:TCGA cohort were utilized.
Recruitment	Research samples were obtained from the Manchester Cancer Research Centre (MCRC) Biobank with informed patient consent obtained prior to sample collection.
Ethics oversight	The MCRC Biobank is licensed by the Human Tissue Authority (license number: 30004) and is ethically approved as a research tissue bank by the South Manchester Research Ethics Committee (Ref: 07/H1003/161+5). The role of the MCRC Biobank is to distribute samples. For more information see www.mcrc.manchester.ac.uk/Biobank/Ethics-and-Licensing .

Note that full information on the approval of the study protocol must also be provided in the manuscript.

Flow Cytometry

Plots

Confirm that:

- The axis labels state the marker and fluorochrome used (e.g. CD4-FITC).
- The axis scales are clearly visible. Include numbers along axes only for bottom left plot of group (a 'group' is an analysis of identical markers).
- All plots are contour plots with outliers or pseudocolor plots.
- A numerical value for number of cells or percentage (with statistics) is provided.

Methodology

Sample preparation	For fluorescent activated cell sorting (FACS) of murine PaFs, a cell suspension was generated by gently lifting the cells using Accutase (Thermo Fisher Scientific) for 5 min at 37°C and following neutralization with DMEM 10% v/v FBS and centrifugation, PaFs were re-suspended in PBS supplemented with 1% v/v FBS, hereafter termed FACS buffer (FB). Cells were then washed and re-suspended in FB supplemented with Fc-block and subjected to surface staining with brilliant violet 421 (BV-421) conjugated anti-CD45 (1:20, BioLegend Clone 30-F11); BV-421 conjugated CD-31 (1:20, BioLegend, clone MEC13.3); BV-421 conjugated Anti-EpCAM (1:20, BioLegend clone G8.8); Phycoerythrin (PE) conjugated CD-90 (1:20 Thermo, clone G7); PE-Cyanine7 (PE-Cy7) conjugated anti-podoplanin (PDPN, 1:20, BioLegend, clone 8.1.1) for 30-45 min on ice, shaking. Following staining, excess antibody was removed using FB, cells were separated using a 70 µm filter (BD) to remove cell-clumps, re-suspended at a concentration of 5 x 10 ⁶ cells/mL in FB and sorted. For FACS of murine iRFP-labelled mPDOs, cells were prepared as single cell suspension using TrypLE, filtered using a 70 µm cell strainer (BD) and retained in AdF Base medium till sorting. iRFP-labelled mPDOs were sorted using an BD™Aria 3 SORP (BD) sorter using the 640 laser and 730/45 filter set.
Instrument	Aria III SORP sorter (BD Biosciences)

Software	BD Diva (BD Biosciences)
Cell population abundance	Only highly positive cells for the selected markers isolated for FACS sorts. The sort was repeated after 7 days of growth to obtain a pure cell population.
Gating strategy	<p>For FACS of murine PaFs, a single-cell gate was first applied and cells were further sorted for BV421- and PE+/PE-Cyanine7+. For FACS purification of iRFP+ mPDOs, a single cell gate was applied and sorted for iRFP (640)+.</p> <p>For CyTOF experiments, the gating strategy has been uploaded with the raw data to https://www.zenodo.org/ under the identifier 10.5281/zenodo.4303962 and can be found in folder: U_2020_F5e-f,SF26,SF27_CyTOF_data.zip/Gating_strategy.pdf.</p>

Tick this box to confirm that a figure exemplifying the gating strategy is provided in the Supplementary Information.